

DSwinIR: Rethinking Window-based Attention for Image Restoration

Gang Wu, *Student Member, IEEE*, Junjun Jiang, *Senior Member, IEEE*, Kui Jiang, *Member, IEEE*, Xianming Liu, *Member, IEEE* and Liqiang Nie, *Senior Member, IEEE*

Abstract—Image restoration has witnessed significant advancements with the development of deep learning models. Especially Transformer-based models, particularly those leveraging window-based self-attention, have become a dominant force in image restoration. However, their performance is fundamentally constrained by the *rigid, non-overlapping window partitioning scheme*, which leads to two critical limitations: insufficient feature interaction across window boundaries and content-agnostic receptive fields that cannot adapt to diverse image structures. Existing methods often rely on heuristic patterns to mitigate these issues, rather than addressing the root cause. In this paper, we propose the Deformable Sliding Window Transformer (DSwinIR), a new foundational backbone architecture that systematically overcomes these limitations. At the heart of DSwinIR is the proposed novel Deformable Sliding Window (DSwin) Attention. This mechanism introduces two fundamental innovations. First, it replaces the rigid partitioning with a token-centric sliding window paradigm, ensuring seamless cross-window information flow and effectively eliminating boundary artifacts. Second, it incorporates a content-aware deformable sampling strategy, which allows the attention mechanism to learn data-dependent offsets and dynamically shape its receptive fields to focus on the most informative image regions. This synthesis endows the model with both strong locality-aware inductive biases and powerful, adaptive long-range modeling capabilities. Extensive experiments show that DSwinIR sets a new state-of-the-art across a wide spectrum of image restoration tasks. For instance, in all-in-one restoration, our DSwinIR surpasses the most recent backbone GridFormer by over 0.53 dB on the three-task benchmark and a remarkable 0.86 dB on the five-task benchmark. The code and pre-trained models are available at <https://github.com/Aitical/DSwinIR>.

Index Terms—All-in-One Image Restoration, Image Deraining, Image Dehazing, Image Denoising, Vision Transformer, Deformable Attention

I. INTRODUCTION

IMAGE restoration, a fundamental and long-standing challenge in computer vision, aims to recover pristine, high-quality images from observations degraded by various factors such as noise, haze, rain, or blur [1]–[4]. In the last decades, the advent of deep learning, particularly Convolutional Neural Networks (CNNs), has heralded a new era in this field, with architectures achieving remarkable performance on specific

G. Wu, J. Jiang, K. Jiang, and X. Liu are with the School of Computer Science and Technology, Harbin Institute of Technology, Harbin 150001, China. E-mail: {gwu@hit.edu.cn, jiangjunjun@hit.edu.cn, jiangkui@hit.edu.cn, csxm@hit.edu.cn}. Corresponding author: Junjun Jiang.

L. Nie is with the School of Computer Science and Technology, Harbin Institute of Technology (Shenzhen), Shenzhen 518055, China. E-mail: {nieliqiang@gmail.com}.

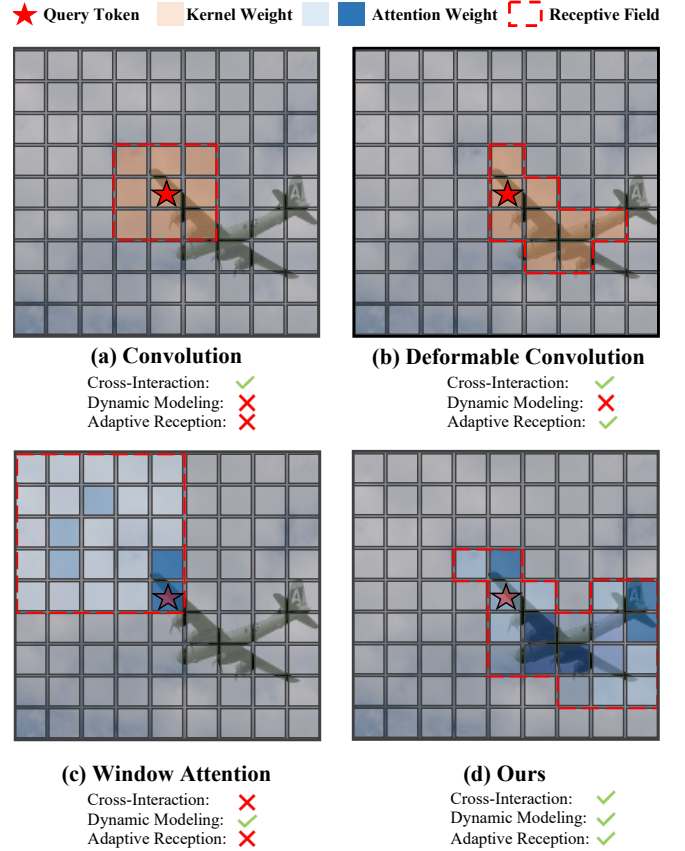


Fig. 1. Comparative analysis of feature extraction mechanisms with an anchor token (marked by \star) as the reference point. (a) Vanilla convolution applies a fixed sampling pattern, leveraging neighborhood features. (b) Deformable convolution introduces adaptive sampling locations based on content, enabling more effective feature integration from relevant regions. (c) Window attention suffers from boundary constraints where anchor tokens near window edges (especially corners) have limited receptive fields, resulting in suboptimal feature extraction. (d) Our proposed Deformable Sliding Window (DSwin) extends window attention with token-centric paradigm and the content-adaptive receptive field, ensuring robust feature aggregation for anchor tokens.

restoration tasks [5], [6]. More recently, Vision Transformers (ViTs) [7] have emerged as a powerful alternative, showcasing exceptional capabilities in modeling long-range dependencies, a crucial aspect for handling complex and spatially extensive degradations.

The practical application of vanilla Transformers to image restoration, however, is hampered by the quadratic computational complexity of the global self-attention mechanism with respect to input resolution. To surmount this obstacle, window-based self-attention, popularized by the Swin Transformer

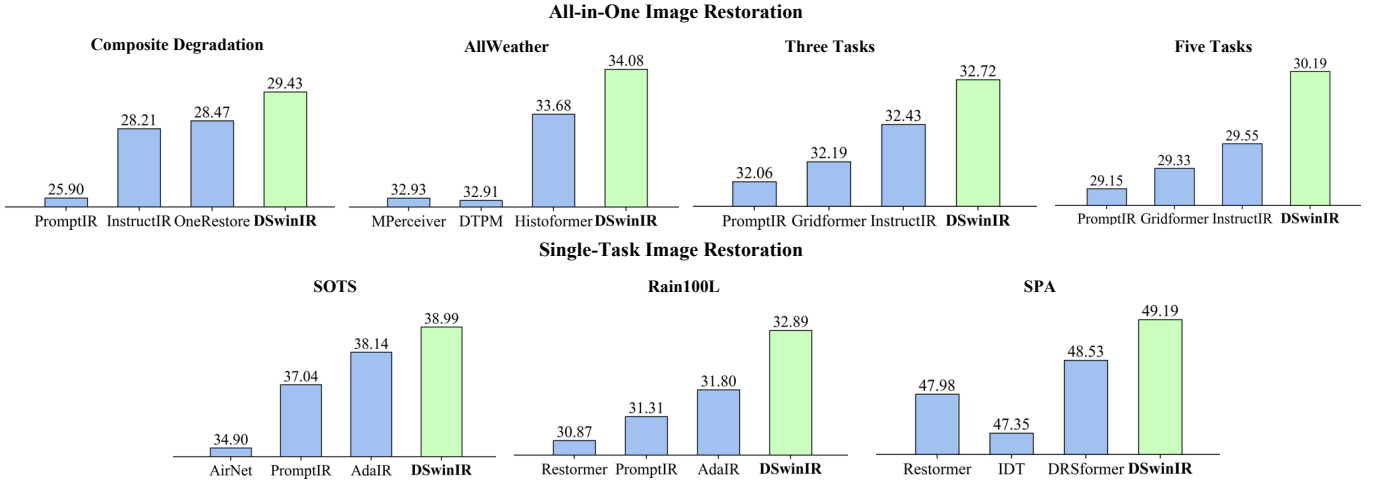


Fig. 2. Quantitative comparison of the proposed DSwinIR against existing methods across diverse image restoration tasks, achieving consistent superior performance. All metrics are reported in PSNR (dB).

[8], has become the *de facto* standard for restoration models like SwinIR [9], and Uformer [10]. By restricting attention computation to small local windows, these models achieve a favorable balance between performance and efficiency. Yet, this very design choice—the rigid, non-overlapping window partition—is also the architecture’s Achilles’ heel. It introduces two fundamental, intertwined limitations: 1) *Boundary Information Truncation*: Tokens near window edges, especially at the corners, have their contextual information severely truncated, leading to suboptimal and spatially-variant feature extraction. 2) *Inflexible Receptive Fields*: The fixed, square-shaped attention pattern is applied uniformly across the image, failing to adapt to the diverse and anisotropic nature of image content and degradation patterns. Several subsequent works have attempted to alleviate these issues. The original Swin Transformer introduced a shifted-window mechanism. Others have proposed more sophisticated, fixed interaction patterns, such as cross-shaped windows [11], axial stripes [12], or sparse token sampling [13]. While these methods have demonstrably improved performance by enhancing inter-window communication, they are essentially *heuristic patches*. They attempt to compensate for one fixed pattern (non-overlapping windows) by introducing other, more complex fixed patterns. They fall short of addressing the core, underlying principle: the shape and scope of an attention field should be dynamically determined by the image content itself, not by a predefined, static template.

In this work, we argue for a principled departure from such heuristic designs. We posit that a truly effective attention mechanism for image restoration must be both *token-centric* and *content-aware*. Inspired by this, we introduce a novel attention mechanism, Deformable Sliding Window (DSwin) Attention, which fundamentally redesigns window-based attention, as illustrated in Fig. 1. First, to address boundary truncation and foster seamless information flow, we embrace a *token-centric sliding window* paradigm. Analogous to the sliding operation of a convolutional kernel, this ensures that every token is at the center of a complete contextual window,

naturally creating overlaps and robustly integrating neighborhood features. Second, to tackle the inflexible receptive field, we introduce a *content-aware deformable mechanism*. Drawing inspiration from deformable convolutions [14], our mechanism learns to predict spatial offsets based on local features, allowing the attention window to dynamically warp and focus on the most salient regions, thus creating effective, data-dependent receptive fields. Building upon this core innovation, we present the Deformable Sliding Window Transformer for Image Restoration (DSwinIR). This new backbone architecture systematically integrates the DSwin attention module, offering a more powerful and flexible foundation for image restoration.

In recent years, the development of all-in-one image restoration models—capable of handling multiple types of degradation within a unified framework—has gained increasing attention. Such models have largely followed two distinct philosophies: one line of work focuses on using task-specific prompts to guide a generic backbone [15], [16], while the other emphasizes evolving the backbone architecture itself to achieve broader restoration capabilities. However, despite the growing interest in prompt-based approaches, we argue that strengthening the backbone architecture remains a fundamental and underexplored avenue. Our work represents a significant advancement for the latter philosophy, demonstrating that a sufficiently powerful and adaptive backbone alone can achieve state-of-the-art performance across diverse tasks, without relying on external prompt-based guidance. This focus on architectural fundamentals is crucial for ensuring both generalization and long-term progress in the field.

We conduct extensive evaluations across diverse image restoration tasks, spanning both all-in-one multiple degradation scenarios and specialized single-task settings. As demonstrated in Fig.2, DSwinIR delivers substantial improvements of 2.1 dB and 1.3 dB in synthetic and real-world deweathering tasks, respectively. Moreover, our approach establishes new state-of-the-art performance on three-task and five-task degradation benchmarks, outperforming previous methods by approximately 0.7 dB and 0.9 dB. For single-task restoration,

DSwinIR surpasses the current leading method DRSformer [13] by 0.62 dB on the challenging real-world deraining SPA dataset [17].

The main contributions of this work are summarized as follows:

- We propose a novel Deformable Sliding Window (DSwin) Attention mechanism. It pioneers a token-centric, content-adaptive paradigm for window-based attention, fundamentally solving the boundary truncation and inflexible receptive field limitations of prior art.
- We develop DSwinIR, a new and powerful backbone architecture for image restoration built upon the DSwin attention module. The architecture cohesively integrates multi-scale feature extraction in both the attention and feed-forward network modules, further enhancing its representation capacity.
- Through extensive experiments on a diverse array of benchmarks, including multi-degradation all-in-one settings and specialized single-task restoration, we demonstrate that DSwinIR consistently and significantly outperforms existing state-of-the-art methods, affirming the superiority of our architectural innovations.

The remainder of this paper is organized as follows. Section II provides a comprehensive review of the image restoration literature, charting the evolution from specialized single-task models to modern all-in-one frameworks. Section III elaborates on our proposed method, detailing the principled progression from the limitations of standard window attention to our novel Deformable Sliding Window (DSwin) attention, and its integration into the complete DSwinIR architecture. Section IV presents extensive experimental validation on a wide array of benchmarks, including quantitative comparisons, qualitative results, in-depth ablation studies. Finally, Section V concludes the paper by summarizing our key contributions and their broader significance for the field.

II. RELATED WORK

Image restoration has evolved from specialized, single-task models to highly versatile all-in-one frameworks. In this section, we chart this evolution to contextualize our contribution. We begin by reviewing the progress in single-task restoration, covering key advancements from the CNN era to the rise of Transformers and other emerging architectures. We then provide a comprehensive analysis of the all-in-one restoration landscape, examining the various innovative strategies developed to tackle multi-degradation scenarios. This analysis will situate our work within the broader field and highlight the unique perspective we bring to architectural design.

A. Single-Task Image Restoration

Deep learning, particularly with the rise of Convolutional Neural Networks (CNNs), has long been the cornerstone of image restoration. Leveraging a data-driven paradigm, CNNs have proven highly effective compared to classical approaches [18], establishing strong foundations in tasks such as image super-resolution [19], image denoising [5], image deraining [20], and image dehazing [21]. Subsequently, a multitude

of more sophisticated studies emerged, for example, models incorporating residual or dense connections [22], [23], as well as those exploring channel attention [24] and non-local attention mechanisms [25]. Within specific domains, landmark contributions have guided the field; for instance, in image deraining, Jiang *et al.* proposed MSPFN [26], which introduced a progressive learning paradigm that inspired a series of subsequent works [27]–[29]. Similarly, image dehazing has also seen many representative studies, such as FFANet [30], and more recent explorations with novel network designs [31], [32]. In parallel, researchers have also focused on developing general restoration architectures applicable to multiple tasks, including MPRNet [33], NAFNet [34], FSNet [35], IRNeXT [36], ConvIR [37], and MB-TaylorFormer [38]. However, these powerful models still typically require separate training for each individual task.

Concurrently, to better model the complex, non-local dependencies often present in degradations, Vision Transformers (ViTs) [7] have garnered significant attention for their powerful dynamic modeling capabilities. While early models like IPT [39] were computationally intensive, the window-based local attention of the Swin Transformer [8] provided an efficient and effective foundation. This spawned a new generation of influential backbones, including SwinIR [9] and Uformer [10]. These advancements were also channeled into powerful task-specific transformers like IDT [40] for image deraining and Dehazeformer [41] for image dehazing. A significant thread of subsequent research has focused extensively on refining the window-based mechanism. For example, HAT [42] enlarged window sizes and used overlaps to enhance cross-window communication, while ELAN [43] and SRFormer [44] addressed computational redundancy. More sophisticated attention patterns were also developed, such as the sparse attention in DRSFormer [13], the strip attention in StripFormer [12], the transposed self-attention in Restormer [45], the integration of an adaptive token dictionary [46], and progressive focused attention [47]. Furthermore, hybrid models like GRL [48] and X-Restormer [49] have explored the fruitful combination of convolutional and attention-based feature extraction.

Alongside these core architectural advancements, several complementary research lines have gained traction. Emerging paradigms like state-space models, exemplified by MambaIR [50], [51], offer a compelling alternative with linear complexity, and Wang *et al.* [52] exploited the vision autoregressive model for all-in-one image restoration. Moreover, researchers are exploring other critical facets of image restoration, such as estimating model uncertainty [53]–[56] and leveraging self-supervised pre-training with contrastive learning to learn robust image priors without paired data [57]–[60]. These diverse efforts collectively enrich the field and provide a strong foundation for tackling more complex restoration scenarios.

B. All-in-One Restoration: The Quest for a Unified Model

Addressing the challenges of all-in-one restoration, where a single model must gracefully handle diverse degradations, has inspired a variety of innovative strategies. A significant body

of work has focused on developing sophisticated prompting mechanisms to guide general-purpose backbones, adapting their behavior to specific tasks. This approach often involves learning adaptive prompts directly from the data. Influential works like AirNet [61] and PromptIR [15] demonstrated how a learned degradation representation can effectively modulate a restoration network. To enhance the discriminability of these prompts, subsequent methods introduced explicit regularization, such as the orthogonality constraints in IDR [62] and the frequency-domain regularization in AdaIR [63]. Others have explored more expressive prompt representations, for instance, by modeling the prompt as a learned distribution as in DPPD [64]. A parallel thread in prompt-based learning injects richer semantic knowledge from large, pre-trained multi-modal models. Methods like DA-CLIP [65], TextualDegRemoval [66], Perceive-IR [67], and OnmiFusion [68] leverage models like CLIP [69] to provide textual or multi-modal guidance. More recently, architectures leveraging Mixture-of-Experts (MoE), such as MoCE-IR [70], have been exploited to select specialized parameters for different restoration tasks.

Complementing the work on prompt-based guidance, other research investigates the optimization challenges inherent in training a single model on diverse data. From a multi-task learning perspective, methods like [71] have explored techniques to mitigate task conflicts, while others like [72] focus on correcting for data and task bias during joint training. Similarly, contrastive learning has been adapted to the all-in-one setting to help the model better decouple degradation-specific features from content-invariant features [73], [74].

C. Positioning Our Contribution

The prevailing trend in all-in-one image restoration has been to build sophisticated prompting superstructures on top of existing, often limited, backbones. Our work diverges from this trend by taking a first-principles approach. We posit that the next significant leap in performance should come not from more complex prompting schemes, but from a fundamental redesign of the attention mechanism at the heart of the backbone. We introduce the Deformable Sliding Window (DSwin) Attention, a new paradigm that is both token-centric and content-aware. It directly addresses the core architectural flaws of prior window-based models by eliminating boundary artifacts and enabling content-adaptive receptive fields. By focusing on evolving the foundational architecture, our DSwinIR demonstrates that a sufficiently intelligent and adaptive backbone can achieve state-of-the-art performance, even surpassing prompt-based methods. Our work does not preclude the use of prompts; rather, it provides a significantly more powerful and robust foundation upon which future, more effective prompting strategies can be built.

III. METHOD

In this section, we present our Deformable Sliding Window Transformer for Image Restoration (DSwinIR). We first provide an overview of the overall network architecture. Then, we elaborate on the heart of our model: the evolution from standard window attention to our proposed Deformable

Sliding Window (DSwin) Attention, detailing its motivation and formulation. Finally, we describe the complete DSwin Transformer Block, which synergistically further extends the DSwin attention with a the practical multi-scale strategy.

A. Overall Architecture

Our architectural design is guided by a philosophy of proven effectiveness and hierarchical feature processing. To this end, we adopt the U-shaped encoder-decoder structure, as illustrated in Fig. 3. The core of this architecture is our novel DSwin Transformer Block, which we will detail in subsequent sections. The entire network is trained end-to-end, optimized with a simple yet robust L_1 pixel-wise loss function, which encourages sharp and accurate predictions by penalizing the absolute difference between the restored output \hat{y} and the ground-truth image y :

$$\mathcal{L} = \|\hat{y} - y\|_1. \quad (1)$$

B. From Window Attention to Deformable Sliding Window Attention

The heart of our work lies in a reconceptualization of window-based attention. In the following subsections, we will introduce this principled evolution, starting from a critical analysis of standard window attention, then introducing our two key innovations—the token-centric sliding mechanism and the content-aware deformable sampling—which together form our final DSwin Attention.

1) Preliminaries: Revisiting Window-based Self-Attention:

To fully appreciate the novelty of our approach, it is essential to first deconstruct the standard window-based self-attention mechanism, as depicted in Fig. 1(c). A query token near the center may enjoy a full set of neighbors, but one at the edge—and especially a corner—is starved of context, blind to potentially crucial information just across the arbitrary window boundary. This “boundary blindness” is the first fundamental flaw we aim to solve. We briefly formalize its operation here to precisely identify the source of its inherent architectural flaws.

Given a 2D input feature map $\mathbf{X} \in \mathbb{R}^{H \times W \times C}$, standard window-based self-attention first partitions \mathbf{X} into a set of non-overlapping windows $\{\mathbf{X}_w\}$, where each window $\mathbf{X}_w \in \mathbb{R}^{M \times M \times C}$ and M is the window size. Within each window, query (\mathbf{Q}_w), key (\mathbf{K}_w), and value (\mathbf{V}_w) projections are computed. The self-attention is then calculated as:

$$\text{Attention}(\mathbf{Q}_w, \mathbf{K}_w, \mathbf{V}_w) = \text{Softmax} \left(\frac{\mathbf{Q}_w \mathbf{K}_w^T}{\sqrt{d}} + \mathbf{B} \right) \mathbf{V}_w, \quad (2)$$

where d is the head dimension and \mathbf{B} is a learnable relative position bias. As discussed in the introduction, this formulation, while efficient, inherently suffers from boundary artifacts and relies on a content-agnostic, fixed receptive field. Consequently, two spatially adjacent tokens that happen to straddle a window boundary are rendered computationally invisible to each other, creating an artificial information bottleneck that prohibits direct interaction.

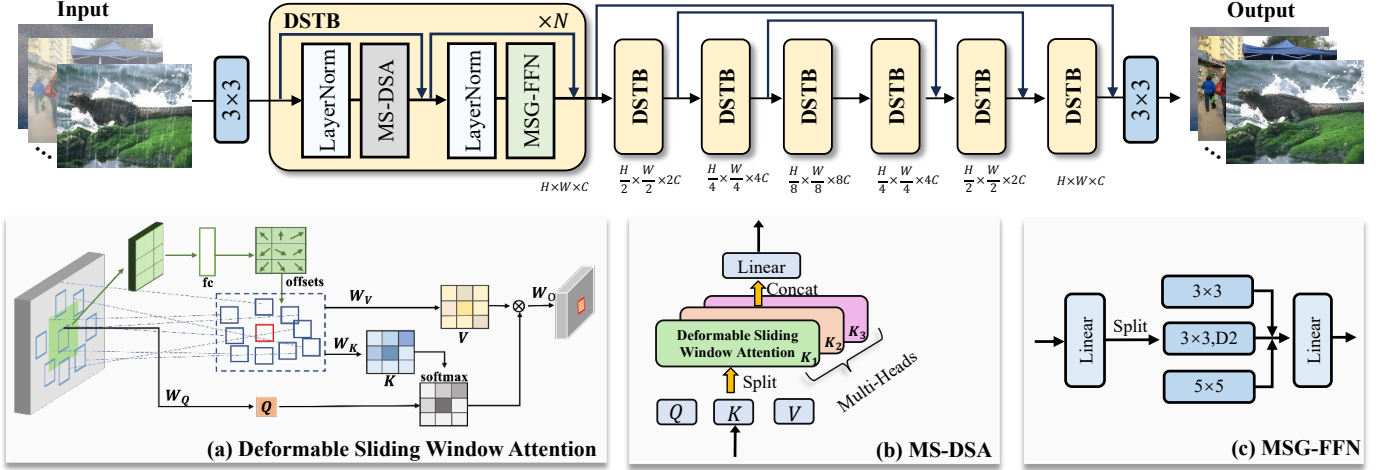


Fig. 3. Overview of the proposed DSwinIR architecture. The model is built upon a U-shaped backbone where the core component is the DSwin Transformer Block (DSTB). The key modules include: (a) The Deformable Sliding Window Attention (DSwin) mechanism, which adaptively samples features by learning content-specific offsets. (b) The Multi-head Self-Attention (MS-DSA) module, which integrates multiple DSwin heads. (c) The Multi-Scale Gated Feed-Forward Network (MSG-FFN), which uses parallel convolutions to enhance feature extraction.

2) *A Token-Centric Paradigm: The Sliding Window Mechanism*: The primary source of boundary artifacts is the window-centric partitioning scheme itself. Therefore, our first key innovation is to abandon this paradigm in favor of a token-centric approach, inspired by the fundamental sliding operation of convolution that has been central to computer vision for decades. Our goal is to ensure that every token in the feature map can serve as the center of its own attention computation, enjoying a complete, uninterrupted contextual neighborhood, much like the sliding operation of a convolution kernel.

For a given query token at position (i, j) , we define its local neighborhood of size $k \times k$. This operation extracts a feature patch $\mathcal{N}_k(i, j) \in \mathbb{R}^{k \times k \times C}$ centered at each position (i, j) . It effectively transforms the feature map \mathbf{X} into a sequence of patches, where each patch contains the keys and values for a corresponding query token. The attention for the query token $\mathbf{q}_{i,j}$ is then computed over the keys $\mathbf{K}_{i,j}$ and values $\mathbf{V}_{i,j}$ extracted from its neighborhood $\mathcal{N}_k(i, j)$:

$$\mathbf{Y}_{i,j}^{\text{slide}} = \sum_{(u,v) \in \mathcal{N}_k} \text{Softmax}_{uv} \left(\frac{\mathbf{q}_{i,j} \cdot \mathbf{k}_{i+u,j+v}}{\sqrt{d}} \right) \mathbf{v}_{i+u,j+v}, \quad (3)$$

where (u, v) are the relative coordinates within the $k \times k$ neighborhood. In stark contrast to the segregated windowing scheme, the local neighborhoods of any two adjacent tokens, such as $\mathbf{q}_{i,j}$ and $\mathbf{q}_{i,j+1}$, now possess a substantial overlap. This shared context explicitly remedies the information bottleneck at artificial boundaries. This sliding mechanism thus naturally creates overlapping receptive fields, ensuring smooth and robust information propagation across all spatial locations.

3) *Content-Aware Sampling: The Deformable Mechanism*: While the sliding window paradigm successfully resolves the boundary problem, its reliance on a rigid, rectilinear grid still represents a significant constraint. This fixed partitioning is fundamentally misaligned with the arbitrary geometry of natural image structures and degradation patterns, such as the fine, diagonal lines of rain streaks or the amorphous, non-uniform

nature of haze. Such a mismatch compromises the model’s ability to efficiently aggregate contextually relevant features, pointing to a critical need for a more flexible mechanism that can dynamically shape its receptive field in a content-aware manner

a) *Offset Prediction and Differentiable Sampling*: For each query token $\mathbf{q}_{i,j}$, we predict a set of 2D spatial offsets $\{\Delta \mathbf{p}_{i,j}^{(u,v)}\}$ for all $k \times k$ sampling points in its neighborhood. These offsets are generated by a lightweight offset prediction network f_θ that takes the query features as input:

$$\{\Delta \mathbf{p}_{i,j}^{(u,v)}\} = f_\theta(\mathbf{q}_{i,j}). \quad (4)$$

The network f_θ is implemented as a depth-wise separable convolution followed by a linear projection, ensuring it remains computationally efficient. The deformed key and value features are then sampled from the original feature map at the new coordinates $(i+u+\Delta u_{i,j}^{(u,v)}, j+v+\Delta v_{i,j}^{(u,v)})$. Since the offsets are fractional, we use *differentiable bilinear interpolation* to sample the features, ensuring the entire process is end-to-end trainable. A value at a fractional location (x, y) is computed as:

$$\mathbf{F}(x, y) = \sum_{i',j'} w(i', j') \cdot \mathbf{X}(\lfloor x \rfloor + i', \lfloor y \rfloor + j'), \quad (5)$$

where $(i', j') \in \{(0, 0), (0, 1), (1, 0), (1, 1)\}$ are the four integer grid neighbors, and $w(i', j')$ are the bilinear interpolation weights, which are proportional to the distance from (x, y) to the opposite corner.

b) *Deformable Sliding Window Attention*: By combining these elements, the final Deformable Sliding Window (DSwin) Attention output for a token at position (i, j) is formulated as:

$$\mathbf{Y}_{i,j} = \sum_{(u,v) \in \mathcal{N}_k} \alpha_{i,j}^{(u,v)} \cdot \mathbf{v}_{\text{interp}}(i+u+\Delta u_{i,j}^{(u,v)}, j+v+\Delta v_{i,j}^{(u,v)}), \quad (6)$$

where $\alpha_{i,j}^{(u,v)}$ represents the attention weights computed using the deformed keys, and $\mathbf{v}_{\text{interp}}$ denotes the value sampled via

TABLE I

COMPREHENSIVE OVERVIEW OF THE EXPERIMENTAL SETTINGS USED TO EVALUATE DSWINIR. EACH SETTING IS DEFINED BY ITS RESTORATION TASKS, DEGRADATION TYPES, AND CORRESPONDING DATASETS FOR TRAINING AND TESTING.

Experiment Settings	Tasks	Degradation Types	Datasets
Three-Task Restoration	3	Denoising, Dehazing, Deraining	BSD400 [75], WED [76], RESIDE (SOTS) [77], Rain100L [78], BSD68 [79]
Five-Task Restoration	5	Adds Motion Deblurring & Low-light Enhancement to the three-task setup	Adds GoPro [80] and LOLv1 [81] to the three-task training set
Synthetic Deweathering	3	Snow, Raindrop, Outdoor Rain	Snow100K [82], Raindrop [83], Outdoor-Rain [84]
Real-World Deweathering	3	Real Rain, Real Snow, Real Haze	SPA-Data [17], RealSnow [85], REVIDE [86]
Composite Degradation	11	Low-light, Haze, Rain, Snow, and their combinations	DIV2K [87] with corresponding degradations

bilinear interpolation. This final formulation, as illustrated in Fig. 1(d), represents a holistic and synergistic solution. It is not merely a sequence of two independent improvements, but a unified paradigm where each component empowers the other. The sliding mechanism lays a robust, boundary-free foundation, ensuring every token has equal access to its local context. Upon this foundation, the deformable mechanism acts with surgical precision, intelligently warping the sampling grid to focus on the most salient information, wherever it may lie. The result is a powerful and expressive attention mechanism that is both structurally sound and semantically aware—perfectly tailored for the complex demands of image restoration.

C. DSwin Transformer Block

The complete DSwin Transformer Block is constructed by integrating our DSwin attention and feedforward network with a complementary multi-scale strategy, which provides much more robust feature extraction.

1) *Multi-Scale DSwin (MS-DSwin) Attention*: Image content and degradations manifest across a spectrum of scales. The standard multi-head attention framework provides a natural and computationally efficient vehicle for capturing such multi-scale information. Instead of treating all attention heads identically, we leverage this structure to explicitly assign different spatial extents to different groups of heads, as depicted in Fig. 3(b).

Specifically, for a model with N heads, we partition them into groups, with each group h being assigned a unique sliding window kernel size k_h . This allows the model to simultaneously aggregate features from both compact local neighborhoods and broader contextual regions within a single MS-DSwin module. The outputs of all heads are then concatenated and passed through a final linear projection, fusing the multi-scale information at negligible extra computational cost.

2) *Multi-Scale Gated Feed-Forward Network (MSG-FFN)*: A standard Feed-Forward Network (FFN) in a Vision Transformer processes each token’s features independently via point-wise linear layers, momentarily losing the rich spatial context captured by the attention layer. To counteract this information bottleneck and maintain a holistic multi-scale design throughout the entire block, we replace the standard FFN with our proposed Multi-Scale Gated FFN (MSG-FFN).

As shown in Fig. 3(c), after an initial channel expansion layer, the MSG-FFN splits the features into parallel branches.

Each branch employs a depth-wise convolution with a different kernel size or dilation rate, explicitly re-introducing spatial reasoning at multiple scales. These parallel features are then passed through a gating mechanism and a final projection layer. This design ensures that both the attention and FFN components of our block actively engage in multi-scale spatial feature processing, creating a more powerful and synergistic architecture.

D. Remarks

It is crucial to position our contribution not as another incremental improvement, but as a fundamental shift in designing attention mechanisms for dense prediction tasks. Previous works often resort to heuristic patches like shifted windows or complex static patterns (e.g., axial stripes, cross-shapes) to mitigate the boundary artifacts of window attention. These methods, however, merely replace one content-agnostic pattern with another, more elaborate one. Our DSwin Attention, in contrast, is a first-principles solution. The token-centric sliding paradigm completely eliminates the concept of a boundary, and the deformable sampling makes the receptive field itself a function of the data. This addresses the core issues of *boundary truncation* and *inflexible receptive fields* directly and dynamically. DSwinIR achieves a more powerful synthesis of the core strengths of CNNs and Transformers.

The prevailing trend in all-in-one restoration has focused on building sophisticated prompting superstructures atop existing, often limited, backbones. The sliding window mechanism re-introduces a strong, locality-aware inductive bias, akin to convolution, which is highly effective for image processing. Simultaneously, the content-aware deformable sampling endows the model with powerful, data-driven adaptivity for long-range modeling, which is the hallmark of attention mechanisms. Our work demonstrates that evolving the foundational architecture itself is a more direct and potent path to state-of-the-art performance.

IV. EXPERIMENTS

In this section, we conduct a comprehensive set of experiments to rigorously evaluate the performance of our proposed DSwinIR. We first detail the experimental setup, including datasets, evaluation protocols, and implementation specifics. We then present extensive quantitative and qualitative comparisons against state-of-the-art methods across a wide range of

TABLE II

QUANTITATIVE COMPARISONS FOR *Setting 1: three distinct degradation tasks*. RESULTS OF OUR PROPOSED DSwinIR ARE IN **BOLD**. * DENOTES THE RESULTS ARE ADOPTED FROM EXISTING WORK [15], [67].

Type	Method	Venue	Denoising (CSD68 [79])			Dehazing	Deraining	Average
			$\sigma = 15$	$\sigma = 25$	$\sigma = 50$	SOTS [77]	Rain100L [78]	
General	MPRNet [6]	CVPR'21	33.27/0.920	30.76/0.871	27.29/0.761	28.00/0.958	33.86/0.958	30.63/0.894
	Restormer [45]	CVPR'22	33.72/0.930	30.67/0.865	27.63/0.792	27.78/0.958	33.78/0.958	30.75/0.901
	NAFNet [34]	ECCV'22	33.03/0.918	30.47/0.865	27.12/0.754	24.11/0.928	33.64/0.956	29.67/0.844
	FSNet* [35]	TPAMI'23	33.81/0.930	30.84/0.872	27.69/0.792	29.14/0.968	35.61/0.969	31.42/0.906
	DRSformer* [13]	CVPR'23	33.28/0.921	30.55/0.862	27.58/0.786	29.02/0.968	35.89/0.970	31.26/0.902
	MambaIR* [50]	ECCV'24	33.88/0.931	30.95/0.874	27.74/0.793	29.57/0.970	35.42/0.969	31.51/0.907
All-in-One	DL [88]	TPAMI'19	33.05/0.914	30.41/0.861	26.90/0.740	26.92/0.391	32.62/0.931	29.98/0.875
	AirNet [61]	CVPR'22	33.92/0.932	31.26/0.888	28.00/0.797	27.94/0.962	34.90/0.967	31.20/0.910
	IDR* [62]	CVPR'23	33.89/0.931	31.32/0.884	28.04/0.798	29.87/0.970	36.03/0.971	31.83/0.911
	PromptIR [15]	NeurIPS'23	33.98/0.933	31.31/0.888	28.06/0.799	30.58/0.974	36.37/0.972	32.06/0.913
	Gridformer* [89]	IJCV'24	33.93/0.931	31.37/0.887	28.11/0.801	30.37/0.970	37.15/0.972	32.19/0.912
	NDR [90]	TIP'24	34.01/0.932	31.36/0.887	28.10/0.798	28.64/0.962	35.42/0.969	31.51/0.910
	InstructIR [16]	ECCV'24	34.15/0.933	31.52/0.890	28.30/0.804	30.22/0.959	37.98/0.978	32.43/0.913
	TextualDegRemoval [66]	CVPR'24	34.01/0.933	31.39/0.890	28.18/0.802	31.63/0.980	37.58/0.979	32.63/0.917
	AdaIR [63]	ICLR'25	34.12/0.935	31.45/0.892	28.19/0.802	31.06/0.980	38.64/0.983	32.69/0.918
	Perceive-IR [67]	TIP'25	34.13/0.934	31.53/0.890	28.31/0.804	30.87/0.975	38.29/0.980	32.63/0.917
	DSwinIR (Ours)	2025	34.12/0.933	31.59/0.890	28.31/0.803	31.86/0.980	37.73/0.983	32.72/0.917

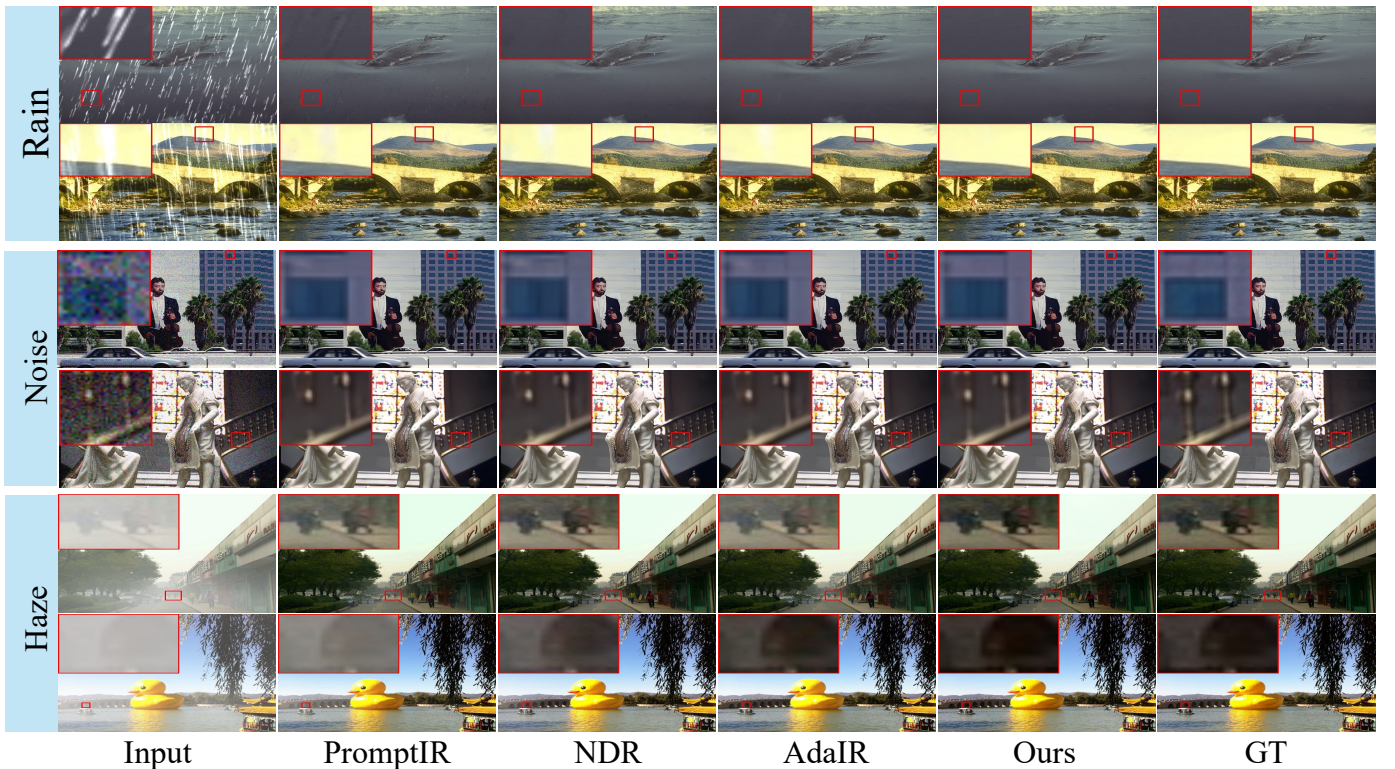


Fig. 4. Visual comparison of restoration results across three degradation tasks: noise removal (top row), rain streak removal (middle row), and dehazing (bottom row). Zoom-in regions (shown in colored boxes) demonstrate that our method achieves superior detail preservation and degradation removal.

image restoration tasks. Finally, we provide in-depth ablation studies to dissect the contribution of each component of our model and analyze its underlying mechanisms.

A. Experimental Setup

To comprehensively validate the capabilities of DSwinIR, we have designed a multi-faceted evaluation protocol spanning

a wide range of restoration scenarios, from standard multi-task benchmarks to complex and composite degradations. This section details the benchmarks, competing methods, and implementation specifics of our experiments.

1) *Evaluation Benchmarks and Metrics*: Our evaluation is structured across four distinct experimental settings, each designed to probe a specific aspect of our model's perfor-

TABLE III
 QUANTITATIVE COMPARISONS FOR *Setting 2: five distinct degradation tasks*. RESULTS OF OUR PROPOSED DSWINIR ARE IN **BOLD**. * DENOTES THE RESULTS ARE ADOPTED FROM PREVIOUS WORK [15], [67].

Type	Method	Venue	Denoising	Dehazing	Deraining	Deblurring	Low-light	Average
			CBSD68 [79]	SOTS [77]	Rain100L [78]	GoPro [80]	LOL [81]	
General	SwinIR [9]	ICCVW'21	30.59/0.868	21.50/0.891	30.78/0.923	24.52/0.773	17.81/0.723	25.04/0.835
	MIRNet-v2 [91]	TPAMI'22	30.97/0.881	24.03/0.927	33.89/0.954	26.30/0.799	21.52/0.815	27.34/0.875
	Restormer [45]	CVPR'22	31.49/0.884	24.09/0.927	34.81/0.962	27.22/0.829	20.41/0.806	27.60/0.881
	NAFNet [34]	ECCV'22	31.02/0.883	25.23/0.939	35.56/0.967	26.53/0.808	20.49/0.809	27.76/0.881
	DRSformer* [13]	CVPR'23	30.97/0.881	24.66/0.931	33.45/0.953	25.56/0.780	21.77/0.821	27.28/0.873
	Retinexformer* [92]	ICCV'23	30.84/0.880	24.81/0.933	32.68/0.940	25.09/0.779	22.76/0.834	27.24/0.873
	FSNet* [35]	TPAMI'23	31.33/0.883	25.53/0.943	36.07/0.968	28.32/0.869	22.29/0.829	28.71/0.898
MambaIR* [50]	ECCV'24	31.41/0.884	25.81/0.944	36.55/0.971	28.61/0.875	22.49/0.832	28.97/0.901	
All-in-One	DL [88]	TPAMI'19	23.09/0.745	20.54/0.826	21.96/0.762	19.86/0.672	19.83/0.712	21.05/0.743
	TAPE [93]	ECCV'22	30.18/0.855	22.16/0.861	29.67/0.904	24.47/0.763	18.97/0.621	25.09/0.801
	Transweather [94]	CVPR'22	29.00/0.841	21.32/0.885	29.43/0.905	25.12/0.757	21.21/0.792	25.22/0.836
	AirNet [61]	CVPR'22	30.91/0.882	21.04/0.884	32.98/0.951	24.35/0.781	18.18/0.735	25.49/0.846
	IDR [62]	CVPR'23	31.60/0.887	25.24/0.943	35.63/0.965	27.87/0.846	21.34/0.826	28.34/0.893
	PromptIR* [15]	NeurIPS'23	31.47/0.886	26.54/0.949	36.37/0.970	28.71/0.881	22.68/0.832	29.15/0.904
	Gridformer* [89]	IJCV'24	31.45/0.885	26.79/0.951	36.61/0.971	29.22/0.884	22.59/0.831	29.33/0.904
	InstructIR [16]	ECCV'24	31.40/0.887	27.10/0.956	36.84/0.973	29.40/0.886	23.00/0.836	29.55/0.907
	AdaIR [63]	ICLR'25	31.35/0.889	30.53/0.978	38.02/0.981	28.12/0.858	23.00/0.845	30.20/0.910
	Perceive-IR [67]	TIP'25	31.44/0.887	28.19/0.964	37.25/0.977	29.46/0.886	22.88/0.833	29.84/0.909
DSwinIR (Ours)	2025	31.34/0.885	30.09/0.975	37.77/0.982	29.17/0.879	22.64/0.843	30.19/0.913	

mance. For all quantitative evaluations, we employ the widely-recognized Peak Signal-to-Noise Ratio (PSNR) and Structural Similarity Index Measure (SSIM). Higher values in both metrics indicate superior restoration quality.

a) Multi-Task All-in-One Restoration: This fundamental setting assesses the ability of a single model to serve as a versatile, general-purpose restorer. Following established conventions, we evaluate on two standard benchmarks. The *three-task* benchmark [15], [61] comprises Gaussian denoising, deraining, and dehazing. The more challenging *five-task* benchmark [63] extends this by incorporating motion deblurring and low-light enhancement, demanding greater generalization from a single set of model weights. The specific datasets for training and testing are detailed in Tab. I.

b) Adverse Weather Removal: This setting focuses on the practical and challenging domain of deweathering. We test DSWinIR's robustness on both synthetic and real-world data. For the synthetic evaluation, we use the "AllWeather" collection [84], which includes images corrupted by snow, raindrops, and heavy rain, allowing for a controlled assessment across varied weather phenomena. To validate real-world efficacy, we employ a challenging benchmark [85] composed of datasets with authentic rain (SPA-Data [17]), snow (RealSnow [85]), and haze (REVIDE [86]), which feature complex, non-uniform artifacts that are the true test of a model's generalization power.

c) Composite Degradation: To push the boundaries of evaluation, we evaluate a composite degradation benchmark introduced in [95] to assess the model's performance in more realistic and complex scenarios where multiple corruptions coexist. This benchmark is crucial for testing a model's ability to disentangle and simultaneously mitigate interacting artifacts. We adopt a challenging test set by combining four

fundamental degradation types: low-light (l), haze (h), rain (r), and snow (s). The evaluation protocol includes all single degradations, all six dual-degradation combinations (e.g., l+h, h+r), and two triple-degradation combinations (l+h+r, l+h+s). Success in this setting signals a higher level of architectural intelligence and robustness.

d) Single-Task Specialization: While all-in-one models demonstrate versatility, a truly superior architecture must also excel when specialized. This experimental setting investigates the "specialization power" of DSWinIR by training it exclusively for a single task. We conduct focused evaluations on image deraining (Rain100L and the real-world SPA-Data) and dehazing (SOTS). Outperforming state-of-the-art specialist models in this context provides unequivocal evidence of our architecture's foundational strength.

2) Compared Methods: To comprehensively position DSWinIR within the literature, we conduct extensive comparisons against a spectrum of state-of-the-art models. This includes foundational, backbone-centric architectures such as Uformer [10], Restormer [45], DRSformer [13], and GridFormer [89], allowing for a direct benchmark of the architectural efficacy of our proposed DSWin attention. Furthermore, we contrast our model with cutting-edge prompt-based and instruction-guided all-in-one methods, including AirNet [61], PromptIR [15], InstructIR [16], and AdaIR [63]. Demonstrating superiority over this class of models highlights that our fundamental architectural innovations provide a more powerful and efficient solution than methods reliant on external semantic guidance or task-specific modules.

3) Implementation Details: DSWinIR is trained end-to-end using the AdamW optimizer with an initial learning rate of 2×10^{-4} , which is decayed using a cosine annealing schedule.

Our model employs a four-level U-shaped architecture, with the number of DSwin Transformer blocks in the encoder stages set to [4, 6, 6, 8] from shallow to deep. We use a batch size of 8 and train on randomly cropped 128×128 patches from the respective training images. All experiments are conducted using PyTorch on NVIDIA 3090 GPUs.

B. Results and Analysis

In this section, we present a detailed analysis of DSwinIR’s performance across a hierarchy of benchmarks, starting from complex multi-degradation scenarios to specialized single-task settings. Our goal is to demonstrate not only the state-of-the-art capabilities of our model but also to dissect the sources of its power.

1) *Dominance in All-in-One Image Restoration*: The most challenging test for any restoration model is the all-in-one setting, where a single network must handle a diverse array of degradations. We evaluate DSwinIR on the standard three-task and five-task benchmarks to demonstrate its capacity as a powerful universal backbone.

a) *Performance on Three Degradation Tasks*: Following the classic benchmark setup [15], [61], we first evaluate on denoising, deraining, and dehazing. The quantitative results are presented in Tab. II. DSwinIR achieves a new state-of-the-art average PSNR of 32.72 dB, consistently outperforming all prior methods. This achievement is significant on two fronts. Firstly, it represents a substantial leap over other foundational architectures like GridFormer (32.19 dB) and DRSformer (31.26 dB), directly validating the efficacy of our DSwin attention in enhancing the intrinsic representation power of the network. Secondly, and perhaps more impressively, this performance is also superior to recent methods that employ additional, non-visual priors. For instance, DSwinIR surpasses the text-guided TextualDegRemoval [66] (32.63 dB) and the instruction-based InstructIR [16] (32.43 dB). That our vision-only backbone can outperform these multi-modal approaches strongly suggests that its architectural intelligence is sufficiently advanced to compensate for, and even exceed, the benefits of external guidance. The qualitative results in Fig. 4 corroborate these findings, showcasing DSwinIR’s superior ability to restore fine textures and remove complex artifacts.

b) *Performance on Five Degradation Tasks*: To further probe the model’s generalization capabilities, we turn to the more demanding five-task benchmark, which introduces deblurring and low-light enhancement. As detailed in Tab. III, DSwinIR again sets a new performance record with an average PSNR of 30.19 dB. The performance gains are particularly striking in tasks requiring significant spatial transformation, such as deraining (+0.93 dB over InstructIR) and dehazing (+2.99 dB over InstructIR). While its performance on low-light enhancement is competitive rather than leading, its exceptional strength across the other tasks secures the best overall average. This highlights the remarkable ability of the DSwinIR architecture to jointly learn from a highly diverse set of degradations within a single set of weights, without catastrophic interference and achieving a new state-of-the-art equilibrium.

2) *Robustness in Deweathering Scenarios*: Beyond general restoration, we investigate DSwinIR’s performance in the specific and practical domain of deweathering, which requires handling complex, real-world atmospheric phenomena.

a) *Synthetic Deweathering Benchmarks*: On the comprehensive AllWeather dataset collection, which includes snow, raindrops, and outdoor rain, DSwinIR demonstrates clear superiority. As presented in Tab. IV, our model achieves an average PSNR of 34.08 dB, surpassing the previous best, Histoformer [104], by a convincing margin of 0.4 dB. The visual results in Fig. 5 are even more compelling. Compared to prior works, including diffusion-based models, DSwinIR consistently produces images with better clarity, more vibrant colors, and sharper details, effectively removing weather artifacts without introducing secondary distortions.

b) *Real-World Deweathering Benchmarks*: The true test of a deweathering model lies in its performance on real-world data. On a challenging benchmark composed of real-world rain, snow, and haze datasets [85], DSwinIR again proves its mettle. As shown in Tab. V, our model achieves an average PSNR of 34.85 dB, significantly outperforming the previous state-of-the-art WGWSNet [85] by 0.84 dB. This robust performance on both synthetic and real-world data underscores the practical applicability and strong generalization of our proposed architecture for tackling adverse weather conditions.

3) *Mastery in Complex Composite Degradations*: The ultimate test of a restoration model’s versatility and power lies in its ability to address composite degradations, where multiple types of corruption are simultaneously present. We evaluate DSwinIR on the challenging composite degradation benchmark, which features 11 combinations of low-light, haze, rain, and snow based on CDD-11 dataset [95]. The quantitative results, presented in Tab. VI, unequivocally demonstrate the dominance of our approach. DSwinIR achieves a new state-of-the-art average PSNR of 29.43 dB, significantly surpassing the next best method, OneRestore [95], by a remarkable margin of 0.98 dB. Even more impressively, this superiority is not merely an average tendency; DSwinIR secures the top performance across *all 11 individual and combined degradation settings*. This consistent, commanding lead is a powerful testament to the robustness and advanced capabilities of our architecture.

In the face of composite degradations like haze and rain, standard attention mechanisms with fixed receptive fields may struggle, either over-smoothing details to remove haze or failing to capture the fine, non-local structure of rain streaks. In contrast, the *deformable* component of DSwin attention allows the model to dynamically tailor its receptive fields, effectively creating task-specific local experts that can, for instance, focus on thin streak-like patterns for deraining while simultaneously attending to broader regions to model and remove haze. Concurrently, the *sliding window* mechanism ensures that this powerful local processing is applied efficiently across the entire feature map, preserving spatial context and preventing the loss of fine-grained texture that can occur when dealing with severe, multi-faceted degradation. This synergy allows DSwinIR to decompose and resolve the complex restoration problem without catastrophic interference between sub-tasks.

These quantitative findings are further substantiated by the

TABLE IV
 QUANTITATIVE COMPARISONS FOR ADVERSE WEATHER REMOVAL INCLUDING RAIN, HAZE, AND SNOW. MISSING VALUES ARE DENOTED BY ‘-’.

Type	Methods	Venue	Snow100K-S [82]		Snow100K-L [82]		Outdoor-Rain [84]		RainDrop [83]		Average	
			PSNR	SSIM	PSNR	SSIM	PSNR	SSIM	PSNR	SSIM	PSNR	SSIM
Task-Specific	SPANet [17]	CVPR’19	29.92	0.8260	23.70	0.7930	-	-	-	-	-	-
	DesnowNet [82]	TIP’18	32.33	0.9500	27.17	0.8983	-	-	-	-	-	-
	HRGAN [96]	CVPR’19	-	-	-	-	21.56	0.8550	-	-	-	-
	MPRNet [6]	CVPR’21	-	-	-	-	28.03	0.9192	-	-	-	-
	AttentiveGAN [83]	CVPR’18	-	-	-	-	-	-	31.59	0.9170	-	-
	IDT [40]	TIP’22	-	-	-	-	-	-	31.87	0.9313	-	-
	NAFNet [34]	ECCV’22	34.79	0.9497	30.06	0.9017	29.59	0.9027	-	-	-	-
	Restormer [45]	CVPR’22	36.01	0.9579	30.36	0.9068	30.03	0.9215	32.18	0.9408	-	-
All-in-One	All-in-One [97]	CVPR’20	-	-	28.33	0.8820	24.71	0.8980	31.12	0.9268	28.05	0.9023
	TransWeather [94]	CVPR’22	32.51	0.9341	29.31	0.8879	28.83	0.9000	30.17	0.9157	30.20	0.9094
	Chen <i>et al.</i> [98]	CVPR’22	34.42	0.9469	30.22	0.9071	29.27	0.9147	31.81	0.9309	31.43	0.9249
	WGWSNet [99]	CVPR’22	34.31	0.9460	30.16	0.9007	29.32	0.9207	32.38	0.9378	31.54	0.9263
	WeatherDiff ₆₄ [100]	TPAMI’23	35.83	0.9566	30.09	0.9041	29.64	0.9312	30.71	0.9312	31.57	0.9308
	WeatherDiff ₁₂₈ [100]	TPAMI’23	35.02	0.9516	29.58	0.8941	29.72	0.9216	29.66	0.9225	31.00	0.9225
	AWRCP [101]	ICCV’23	36.92	0.9652	31.92	0.9341	31.39	0.9329	31.93	0.9314	33.04	0.9409
	GridFormer [89]	IJCV’24	37.46	0.9640	31.71	0.9231	31.87	0.9335	32.39	0.9362	33.36	0.9392
	MPerceiver [102]	CVPR’24	36.23	0.9571	31.02	0.9164	31.25	0.9246	33.21	0.9294	32.93	0.9319
	DTPM [103]	CVPR’24	37.01	0.9663	30.92	0.9174	30.99	0.9340	32.72	0.9440	32.91	0.9404
	Histoformer [104]	ECCV’24	<u>37.41</u>	<u>0.9656</u>	<u>32.16</u>	<u>0.9261</u>	<u>32.08</u>	<u>0.9389</u>	<u>33.06</u>	<u>0.9441</u>	<u>33.68</u>	<u>0.9437</u>
	DSwinIR (Ours)	2025	38.11	0.9683	32.58	0.9312	32.76	0.9502	32.88	0.9474	34.08	0.9493

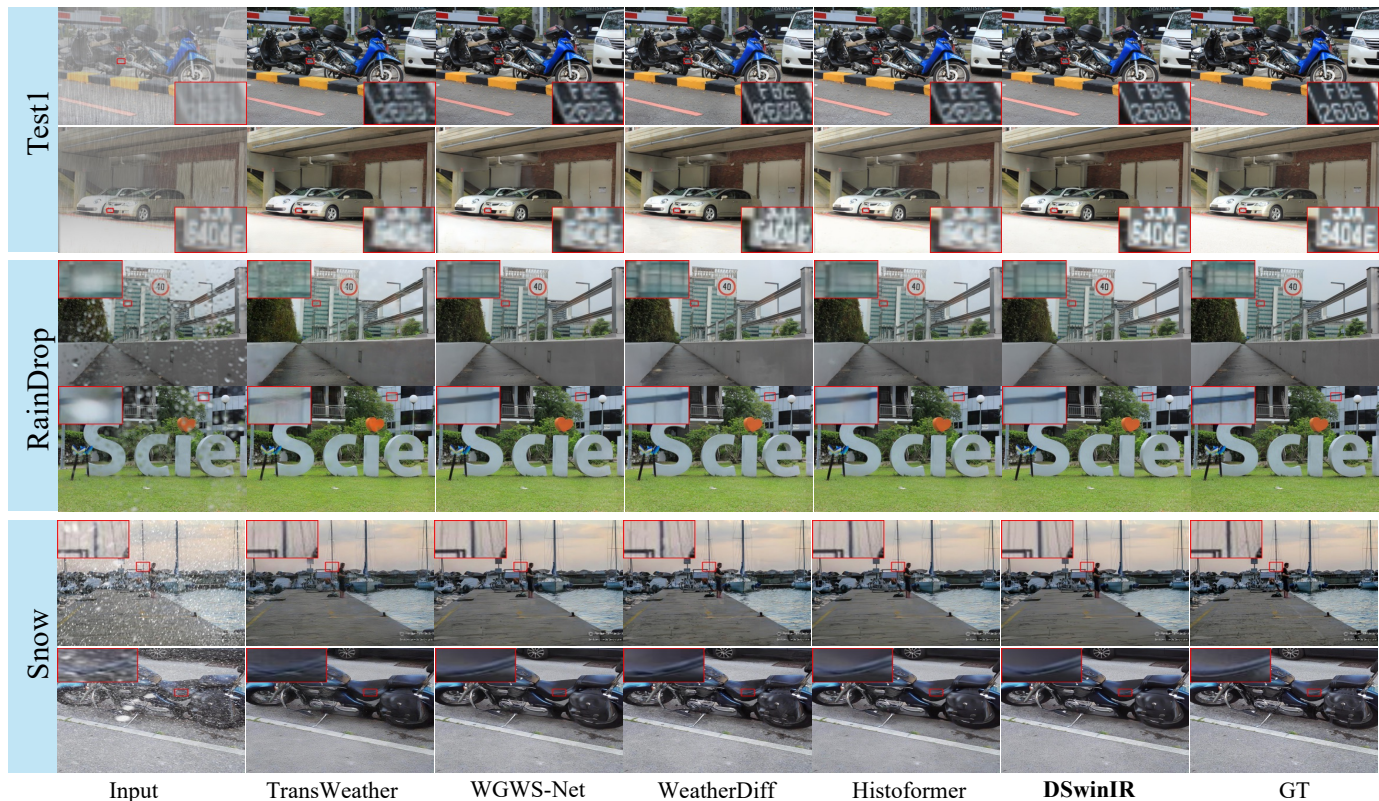


Fig. 5. Vision results of AllWeather datasets, from up to bottom is samples for outdoor-rain, raindrop and snow test data. Our DSwinIR achieves better clarity even compared to the diffusion-based approaches.

qualitative results shown in Fig. 6. The visual examples highlight DSwinIR’s superior ability to restore clarity and detail in images afflicted by multiple interacting degradations. Our model more effectively removes all traces of weather

artifacts while simultaneously enhancing brightness and contrast, achieving perceptually more natural and artifact-free results. This confirms that DSwinIR’s architectural advantages translate directly into visually compelling and high-fidelity

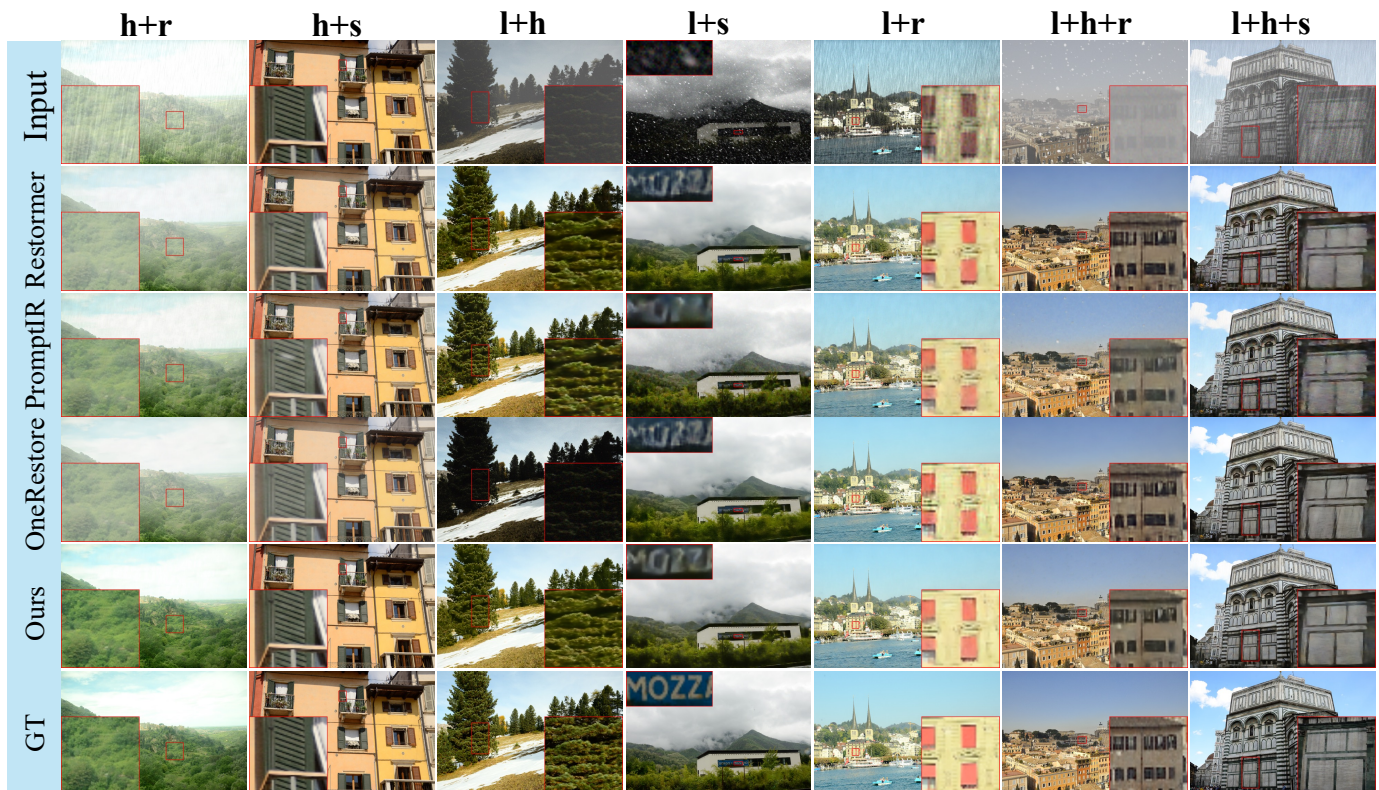


Fig. 6. Visual results on the composite degradation tasks, showcasing performance on mixed degradations. Our method more effectively mitigates multiple interacting degradations, restoring clearer images with improved color fidelity and detail.

TABLE V
COMPARISON ON DE-WEATHERING TASKS ON REAL-WORLD DATASETS
FOLLOWING [85]

Datasets	Methods	PSNR \uparrow	SSIM \uparrow
SPA+	Chen et al. [98]	37.32	0.97
	WGWSNet [85]	38.94	0.98
	TransWeather [94]	33.64	0.93
	DSwinIR (Ours)	40.60	0.98
RealSnow	Chen et al. [98]	29.37	0.88
	WGWSNet [85]	29.46	0.85
	TransWeather [94]	29.16	0.82
	DSwinIR (Ours)	33.80	0.93
REVIDE	Chen et al. [98]	20.10	0.85
	WGWSNet [85]	20.44	0.87
	TransWeather [94]	17.33	0.82
	DSwinIR (Ours)	30.14	0.89
Average	Chen et al. [98]	28.93	0.90
	WGWSNet [85]	29.61	0.90
	TransWeather [94]	26.71	0.86
	DSwinIR (Ours)	34.85	0.93

image restoration.

4) *Specialization Power in Single-Task Settings*: A defining characteristic of a truly superior architecture is its ability to excel not only as a generalist but also as a specialist. To investigate this “specialization power”, we adapt DSwinIR for single-task training on standard deraining and dehazing benchmarks. These experiments are critical to demonstrate

that the performance of our foundational design is not diluted but can be concentrated to achieve mastery, rivaling and even surpassing models designed exclusively for these tasks.

a) *Deraining on Rain100L*: We begin with the standard Rain100L benchmark. As shown in Tab. VII, the field is highly competitive. When trained solely for this task, DSwinIR establishes a new state-of-the-art result. The performance leap over strong backbone architectures like Restormer (+1.98 dB) is substantial, reaffirming the architectural progress our DSwin attention provides. More tellingly, DSwinIR also narrowly surpasses the latest top-performing model, AdaIR, by 0.12 dB. In a mature benchmark where gains are often incremental, achieving the top position provides unequivocal evidence of DSwinIR’s high-fidelity reconstruction capabilities when fully specialized.

b) *Dehazing on SOTS Outdoor*: The task of single-image dehazing presents a different challenge, often requiring a nuanced understanding of global atmospheric light and local object details. Here, the advantages of DSwinIR’s design become profoundly apparent. As detailed in Tab. VIII, DSwinIR achieves a PSNR of 32.89 dB. This is not merely an incremental improvement but a massive leap in performance, surpassing the powerful AdaIR by an impressive 1.09 dB. This substantial margin is a direct testament to the efficacy of our DSwin attention. We posit that the deformable mechanism’s ability to adapt its receptive field to non-homogenous haze, combined with the sliding mechanism’s capacity to preserve fine structural details, creates a perfect synergy for this task. This result strongly validates that our architectural principles

TABLE VI
QUANTITATIVE RESULTS ON THE COMPOSITE DEGRADATION SETTING. OUR RESULTS ARE HIGHLIGHTED IN **BOLD**, AND THE BEST RESULTS ARE UNDERLINED.

Method	Venue	l	h	r	s	l+h	l+r	l+s	h+r	h+s	l+h+r	l+h+s	Avg.
Restormer [45]	CVPR'22	26.29	28.35	33.10	33.43	24.80	25.28	24.99	26.80	26.15	23.90	23.82	26.99
NAFNet [34]	ECCV'22	24.50	25.34	29.24	29.54	21.91	22.75	22.79	23.67	23.86	21.03	20.82	24.13
AirNet [61]	CVPR'22	24.83	24.21	26.55	26.79	23.23	22.82	23.29	22.21	23.29	21.80	22.24	23.75
PromptIR [15]	NeurIPS'23	26.32	26.10	31.56	31.53	24.49	25.05	24.51	24.54	23.70	23.74	23.33	25.90
TransWeather [94]	CVPR'22	23.39	23.95	26.69	25.74	22.24	22.62	21.80	23.10	22.34	21.55	21.01	23.13
WeatherDiff [85]	TPAMI'23	23.58	21.99	24.85	24.80	21.83	22.69	22.12	21.25	21.99	21.23	21.04	22.49
WGWSNet [85]	CVPR'23	24.39	27.90	33.15	34.43	24.27	25.06	24.60	27.23	27.65	23.90	23.97	26.96
InstructIR [16]	ECCV'24	26.70	32.61	33.51	34.45	24.36	25.41	25.63	28.80	29.64	24.84	24.32	28.21
OneRestore [95]	ECCV'24	26.55	32.71	33.48	34.50	26.15	25.83	25.56	30.27	30.46	25.18	25.28	28.47
DSwinIR (Ours)	2025	<u>27.38</u>	<u>33.72</u>	<u>34.95</u>	<u>35.44</u>	<u>26.56</u>	<u>26.54</u>	<u>26.24</u>	<u>30.94</u>	<u>30.54</u>	<u>25.70</u>	<u>25.70</u>	<u>29.43</u>

TABLE VII
SINGLE-TASK DERAINING RESULTS ON THE RAIN100L DATASET. DSWINIR ESTABLISHES A NEW STATE-OF-THE-ART, DEMONSTRATING ITS HIGH SPECIALIZATION POTENTIAL.

Method	DIDMDN [105]	UMR [106]	SIRR [107]	MSPFN [26]	LPNet [108]	AirNet [61]	Restormer [45]	PromptIR [15]	AdaIR [63]	DSwinIR (Ours)
PSNR	23.79	32.39	32.37	33.50	33.61	34.90	36.74	37.04	38.90	39.02
SSIM	0.773	0.921	0.926	0.948	0.958	0.977	0.978	0.979	0.985	0.986

are particularly well-suited for tackling complex, spatially-variant degradations.

c) *Real-World Deraining on SPA-Data*: Finally, we test DSwinIR’s specialization power against the ultimate challenge: complex, non-uniform artifacts in real-world images. We use the SPA-Data benchmark, known for its realistic and challenging rain streak patterns. The results, summarized in Tab. IX, are striking. DSwinIR achieves a PSNR of 49.19 dB, establishing a new state-of-the-art. Most notably, it outperforms the highly-optimized and specialized deraining model, DRSformer, by a significant margin of 0.66 dB. Thriving in such a complex, real-world environment, where degradation patterns defy simple synthetic models, is powerful proof of the robustness and superior modeling capacity of the DSwin attention mechanism. It validates that our model’s ability to learn adaptive, data-driven receptive fields is not just a theoretical advantage but a practical necessity for tackling real-world image restoration.

C. Ablation Study

To validate our design choices and rigorously quantify the contribution of each proposed component, we conduct a series of in-depth ablation studies. We use the challenging three-task all-in-one setting as our testbed and present the comprehensive results in Fig. 7. Our analysis proceeds methodically, first deconstructing the core DSwin attention mechanism and then justifying the configuration of the full DSwinIR block.

a) *Efficacy of the Core DSwin Mechanisms*: The central thesis of our work is that simultaneously resolving the boundary limitations and the static receptive field issue is key to unlocking superior performance. To prove this, we begin with strong backbone baselines and incrementally introduce our core ideas. The Uformer [10] and DRSformer [13] baselines

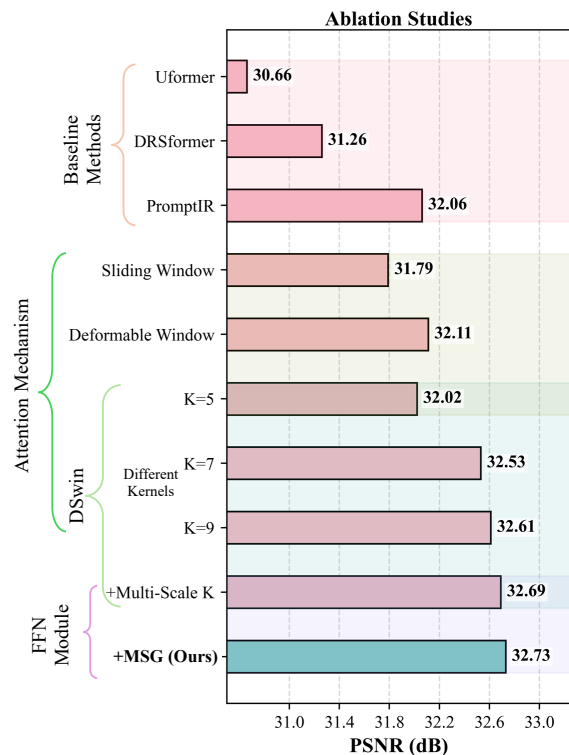


Fig. 7. Ablation studies demonstrating the effectiveness of our key components. We evaluate (1) different attention mechanisms, showing improvements from Sliding Window (31.79 dB) and Deformable Window (32.11 dB) over baselines; (2) DSwin configurations with various kernel sizes ($K=5, 7, 9$) and Multi-scale enhancement (32.69 dB); and (3) FFN module with MSG enhancement, achieving the best performance (32.73 dB). All experiments report the average PSNR of three distinct degradation tasks.

establish a performance benchmark of 30.66 dB and 31.26 dB, respectively. Our first experiment, isolating the sliding window

TABLE VIII

SINGLE-TASK DEHAZING RESULTS ON THE SOTS OUTDOOR TEST SET. DSWINIR DEMONSTRATES A SIGNIFICANT PERFORMANCE LEAP OVER ALL PRIOR METHODS.

Method	DehazeNet [21]	MSCNN [109]	AODNet [110]	EPDN [111]	FDGAN [112]	AirNet [61]	Restormer [45]	PromptIR [15]	AdaIR [63]	DSwinIR (Ours)
PSNR	22.46	22.06	20.29	22.57	23.15	23.18	30.87	31.31	31.80	32.89
SSIM	0.851	0.908	0.877	0.863	0.921	0.900	0.969	0.973	0.981	0.984

TABLE IX

SINGLE-TASK DERAISING RESULTS ON THE REAL-WORLD SPA-DATA DATASET. DSWINIR SIGNIFICANTLY OUTPERFORMS EVEN HIGHLY SPECIALIZED DERAISING MODELS.

Method	MSPFN [26]	MPRNet [33]	DualGCN [113]	SPDNet [114]	Uformer [10]	Restormer [45]	IDT [40]	DRSformer [13]	DSwinIR (Ours)
PSNR	43.43	43.64	44.18	43.20	46.13	47.98	47.35	48.53	49.19
SSIM	0.9843	0.9844	0.9902	0.9871	0.9913	0.9921	0.9930	0.9924	0.9938

TABLE X

EFFICIENCY EVALUATION OF DIFFERENT METHODS WITH 256×256 INPUT.

Methods	Core Operation	Params.	FLOPs	Latency	PSNR
AirNet [61]	Deformable Conv	9M	301G	0.57s	31.20
Uformer [10]	Window Attention	20M	41G	0.45s	30.66
Restormer [45]	Transposed Self-Attention	26M	155G	0.67s	30.75
PromptIR [15]	Trans. SA + Prompts	36M	173G	0.71s	32.06
DRSformer [13]	Sparse Window Attention	33M	243G	0.82s	31.26
DSwinIR (Ours)	DSwin Attention	24M	147G	0.55s	32.72

mechanism, yields a performance of 31.79 dB. This substantial gain over a comparable backbone structure confirms that simply enabling smooth information flow across all spatial locations by adopting a token-centric paradigm provides a powerful performance uplift. In a parallel experiment, isolating the deformable window mechanism boosts the PSNR to an even higher 32.11 dB, even surpassing the prompt-based PromptIR baseline. This result underscores the immense value of a content-adaptive receptive field that can focus on salient features. The true power of our design is revealed when these two concepts are combined. The resulting DSwin module (e.g., with $K=7$) achieves 32.53 dB, a gain that is markedly greater than the sum of the individual improvements. This demonstrates a powerful synergistic effect: the sliding mechanism provides robust structural context, which in turn provides a better feature foundation for the deformable mechanism to learn meaningful semantic offsets.

b) Effective Receptive Field and Efficiency: The visualizations of the receptive field in Fig. 8 offer profound qualitative insights into why DSwinIR is so effective. Its receptive field is demonstrably both global in reach and local in precision. This is the direct result of our design principles: the sliding mechanism ensures a connected, expansive base, while the deformable mechanism learns to dynamically concentrate attention on areas like object contours and textures.

Moreover, DSwinIR also exhibits exceptional computational efficiency, as detailed in Tab. X. It is crucial to note that DSwinIR achieves its state-of-the-art performance not through brute force, but through superior architectural design. Compared to its top-performing competitors, DSwinIR is significantly more economical. For instance, it requires 15% fewer FLOPs and is 22% faster than PromptIR, while delivering a substantially higher PSNR. The advantage is even more dra-

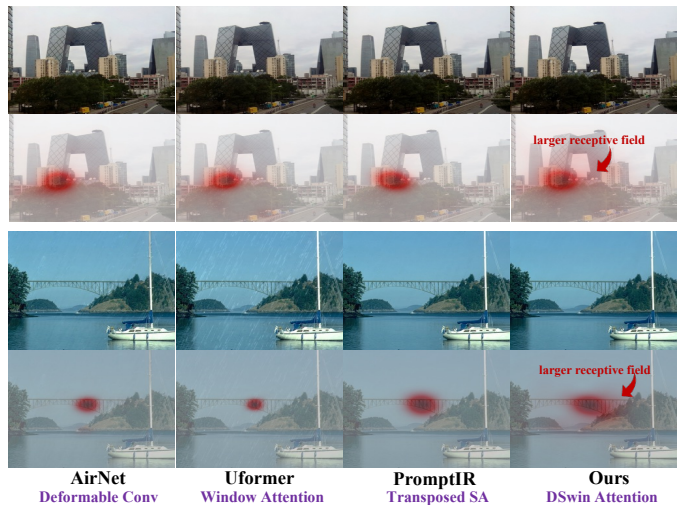


Fig. 8. Visualization of receptive fields of multiple backbones by LAM [115].

matic when compared to DRSformer, against which DSwinIR uses a staggering 40% fewer FLOPs. This potent combination of a more intelligent mechanism and superior computational efficiency establishes DSwinIR not merely as another high-performing model, but as a fundamentally more advanced and practical architecture for the field of image restoration.

c) Impact of Kernel Size and Multi-Scale Strategy:

Having validated the DSwin concept, we next investigate its optimal configuration. We first analyze the impact of a fixed kernel size, testing $K=5$, $K=7$, and $K=9$. The results show a clear trend: performance improves from 32.02 dB ($K=5$) to 32.53 dB ($K=7$), and then begins to plateau at 32.61 dB ($K=9$). This suggests a trade-off, where a larger receptive field is beneficial, but excessively large kernels may not provide proportionally greater returns for their computational cost. This observation motivates our multi-scale strategy. By employing multi-scale kernels within a single attention module (+Multi-Scale K), we reach a PSNR of 32.69 dB. This result is superior to even the best-performing single-kernel model ($K=9$), providing clear evidence that empowering the model to simultaneously perceive features at multiple scales is more effective than relying on a single, large-but-fixed receptive field.

d) *Contribution of the Multi-Scale Gated FFN*: The final step in our analysis is to justify the design of the feed-forward network. By incorporating our proposed multi-scale gated FFN (+MSG), the model’s performance reaches its peak at 32.73 dB. While the incremental gain at this stage is modest, its importance is strategic. It confirms that maintaining a holistic multi-scale philosophy across the *entire* Transformer block—in both the attention module and the FFN—is beneficial. This creates a cohesive and synergistic architecture where features are consistently processed and refined across a spectrum of spatial extents, leading to the final state-of-the-art performance. The combination of all these validated components results in our final DSwinIR model.

D. Discussion and Limitation

The extensive experiments in this paper provide strong validation for our core thesis: a first-principles evolution of the backbone architecture is a direct and potent path to advancing all-in-one image restoration. Our proposed DSwinIR, built upon the novel Deformable Sliding Window attention, consistently established a new state-of-the-art across a wide range of benchmarks, often outperforming even sophisticated prompt-guided systems. This superiority is most pronounced in its massive performance leaps on tasks with spatially-variant degradations, such as dehazing and real-world deraining. We attribute this success to the synergistic combination of the token-centric sliding mechanism, which eradicates boundary artifacts, and the content-aware deformable sampling, which creates adaptive, non-rigid receptive fields. This unique capability allows DSwinIR to effectively model complex degradation patterns that are intractable for methods relying on static attention schemes, confirming the power of our architectural redesign.

Despite its demonstrated strengths, our work also illuminates several promising avenues for future research. First, while our architecture excels at restoring spatial structure, its performance on tasks dominated by extreme photometric adjustments, such as low-light enhancement, is competitive rather than leading. Future work could explore hybrid approaches that combine our powerful backbone with specialized modules for global color mapping. Second, our focus on architectural innovation means adapting DSwinIR to new tasks requires full retraining. A compelling direction is to integrate our backbone with parameter-efficient fine-tuning (PEFT) techniques, creating systems that are both powerful and highly adaptable. Finally, we believe the core principles of token-centric, content-adaptive attention hold significant potential beyond restoration, offering a promising new building block for other dense prediction tasks like semantic segmentation and object detection, where the ability to dynamically model features is paramount.

V. CONCLUSION

In this paper, we challenged the prevailing paradigm of window-based self-attention, arguing that its rigid, non-overlapping partitioning scheme imposes fundamental limitations on performance in image restoration. We introduced

the Deformable Sliding Window Transformer (DSwinIR), a new foundational architecture built upon our novel DSwin attention mechanism. By pioneering a token-centric, content-aware paradigm that synergistically combines a sliding window to eliminate boundary artifacts with a deformable mechanism to learn adaptive receptive fields, DSwinIR achieves a more powerful and principled approach to visual feature representation. Extensive experiments rigorously demonstrated that this architectural evolution translates directly into substantial performance gains, establishing new state-of-the-art results across a diverse array of all-in-one and single-task restoration benchmarks. Ultimately, this work validates the critical importance of advancing fundamental architectures and offers a powerful new building block that we hope will inspire future developments in image restoration and beyond.

REFERENCES

- [1] Michael Elad, Bahjat Kwar, and Gregory Vaksman. Image denoising: The deep learning revolution and beyond - A survey paper. *SIAM J. Imaging Sci.*, 16(3):1594–1654, 2023.
- [2] Jie Gui, Xiaofeng Cong, Yuan Cao, Wenqi Ren, Jun Zhang, Jing Zhang, Jiuxin Cao, and Dacheng Tao. A comprehensive survey and taxonomy on single image dehazing based on deep learning. *ACM Comput. Surv.*, 55(13s), 2023.
- [3] Xiang Chen, Jinshan Pan, Jiangxin Dong, and Jinhui Tang. Towards unified deep image deraining: A survey and A new benchmark. *CoRR*, abs/2310.03535, 2023.
- [4] Kaihao Zhang, Wenqi Ren, Wenhan Luo, Wei-Sheng Lai, Björn Stenger, Ming-Hsuan Yang, and Hongdong Li. Deep image deblurring: A survey. *Int. J. Comput. Vis.*, 130(9):2103–2130, 2022.
- [5] Kai Zhang, Wangmeng Zuo, Yunjin Chen, Deyu Meng, and Lei Zhang. Beyond a gaussian denoiser: Residual learning of deep cnn for image denoising. *IEEE Trans. Image Process.*, 26(7):3142–3155, 2017.
- [6] Syed Waqas Zamir, Aditya Arora, Salman H. Khan, Munawar Hayat, Fahad Shahbaz Khan, Ming-Hsuan Yang, and Ling Shao. Multi-stage progressive image restoration. In *Proceedings of the IEEE/CVF Conference on Computer Vision and Pattern Recognition (CVPR)*, pages 14821–14831, 2021.
- [7] Alexey Dosovitskiy, Lucas Beyer, Alexander Kolesnikov, Dirk Weissenborn, Xiaohua Zhai, Thomas Unterthiner, Mostafa Dehghani, Matthias Minderer, Georg Heigold, Sylvain Gelly, Jakob Uszkoreit, and Neil Houlsby. An image is worth 16x16 words: Transformers for image recognition at scale. In *Proceedings of Proceedings of International Conference on Learning Representations (ICLR)*, 2021.
- [8] Ze Liu, Yutong Lin, Yue Cao, Han Hu, Yixuan Wei, Zheng Zhang, Stephen Lin, and Baining Guo. Swin transformer: Hierarchical vision transformer using shifted windows. In *IEEE/CVF International Conference on Computer Vision (ICCV)*, pages 9992–10002, 2021.
- [9] Jingyun Liang, Jiezhang Cao, Guolei Sun, Kai Zhang, Luc Van Gool, and Radu Timofte. SwinIR: Image restoration using swin transformer. In *IEEE/CVF International Conference on Computer Vision (ICCV) Workshops*, pages 1833–1844, 2021.
- [10] Zhendong Wang, Xiaodong Cun, Jianmin Bao, Wengang Zhou, Jianzhuang Liu, and Houqiang Li. Uformer: A general u-shaped transformer for image restoration. In *Proceedings of IEEE/CVF Conference on Computer Vision and Pattern Recognition (CVPR)*, pages 17662–17672, 2022.
- [11] Zheng Chen, Yulun Zhang, Jinjin Gu, Yongbing Zhang, Linghe Kong, and Xin Yuan. Cross aggregation transformer for image restoration. In *Proceedings of Advances in Neural Information Processing Systems (NeurIPS)*, 2022.
- [12] Fu-Jen Tsai, Yan-Tsung Peng, Yen-Yu Lin, Chung-Chi Tsai, and Chia-Wen Lin. Stripformer: Strip transformer for fast image deblurring. In *Proceedings of European Conference on Computer Vision (ECCV)*, volume 13679, pages 146–162, 2022.
- [13] Xiang Chen, Hao Li, Mingqiang Li, and Jinshan Pan. Learning a sparse transformer network for effective image deraining. In *Proceedings of IEEE/CVF Conference on Computer Vision and Pattern Recognition (CVPR)*, pages 5896–5905, 2023.

- [14] Jifeng Dai, Haozhi Qi, Yuwen Xiong, Yi Li, Guodong Zhang, Han Hu, and Yichen Wei. Deformable convolutional networks. In *IEEE/CVF International Conference on Computer Vision (ICCV)*, pages 764–773. IEEE Computer Society, 2017.
- [15] Vaishnav Potlapalli, Syed Waqas Zamir, Salman H. Khan, and Fahad Shahbaz Khan. Promptir: Prompting for all-in-one image restoration. In *Proceedings of Advances in Neural Information Processing Systems (NeurIPS)*, 2023.
- [16] Marcos V Conde, Gregor Geigle, and Radu Timofte. High-quality image restoration following human instructions. In *Proceedings of European Conference on Computer Vision (ECCV)*, pages 1–12, 2024.
- [17] Tianyu Wang, Xin Yang, Ke Xu, Shaozhe Chen, Qiang Zhang, and Rynson W. H. Lau. Spatial attentive single-image deraining with a high quality real rain dataset. In *Proceedings of the IEEE/CVF Conference on Computer Vision and Pattern Recognition (CVPR)*, pages 12270–12279, 2019.
- [18] M.R. Banham and A.K. Katsaggelos. Digital image restoration. *IEEE Signal Processing Magazine*, 14(2):24–41, 1997.
- [19] Chao Dong, Chen Change Loy, Kaiming He, and Xiaoou Tang. Image super-resolution using deep convolutional networks. *IEEE Trans. Pattern Anal. Mach. Intell.*, 38(2):295–307, 2016.
- [20] Xueyang Fu, Jiabin Huang, Xinghao Ding, Yinghao Liao, and John W. Paisley. Clearing the skies: A deep network architecture for single-image rain removal. *IEEE Trans. Image Process.*, 26(6):2944–2956, 2017.
- [21] Bolun Cai, Xiangmin Xu, Kui Jia, Chunmei Qing, and Dacheng Tao. Dehazenet: An end-to-end system for single image haze removal. *IEEE Trans. Image Process.*, 25(11):5187–5198, 2016.
- [22] Bee Lim, Sanghyun Son, Heewon Kim, Seungjun Nah, and Kyoung Mu Lee. Enhanced deep residual networks for single image super-resolution. In *Proceedings of IEEE/CVF Conference on Computer Vision and Pattern Recognition (CVPR) Workshops*, pages 1132–1140, 2017.
- [23] Yulun Zhang, Yapeng Tian, Yu Kong, Bineng Zhong, and Yun Fu. Residual dense network for image super-resolution. In *Proceedings of IEEE/CVF Conference on Computer Vision and Pattern Recognition (CVPR)*, pages 2472–2481, June 2018.
- [24] Yulun Zhang, Kunpeng Li, Kai Li, Lichen Wang, Bineng Zhong, and Yun Fu. Image super-resolution using very deep residual channel attention networks. In *Proceedings of European Conference on Computer Vision (ECCV)*, pages 294–310, 2018.
- [25] Yiqun Mei, Yuchen Fan, and Yuqian Zhou. Image super-resolution with non-local sparse attention. In *Proceedings of the IEEE/CVF Conference on Computer Vision and Pattern Recognition (CVPR)*, pages 3517–3526, 2021.
- [26] Kui Jiang, Zhongyuan Wang, Peng Yi, Chen Chen, Baojin Huang, Yimin Luo, Jiayi Ma, and Junjun Jiang. Multi-scale progressive fusion network for single image deraining. In *Proceedings of IEEE/CVF Conference on Computer Vision and Pattern Recognition (CVPR)*, pages 8346–8355, 2020.
- [27] Siqi Ni, Xueyun Cao, Tao Yue, and Xuemei Hu. Controlling the rain: From removal to rendering. In *Proceedings of IEEE/CVF Conference on Computer Vision and Pattern Recognition (CVPR)*, pages 6328–6337, 2021.
- [28] Man Zhou, Jie Xiao, Yifan Chang, Xueyang Fu, Aiping Liu, Jinshan Pan, and Zheng-Jun Zha. Image de-raining via continual learning. In *Proceedings of IEEE/CVF Conference on Computer Vision and Pattern Recognition (CVPR)*, pages 4907–4916, 2021.
- [29] Xiang Chen, Jinshan Pan, and Jiangxin Dong. Bidirectional multi-scale implicit neural representations for image deraining. In *Proceedings of IEEE/CVF Conference on Computer Vision and Pattern Recognition (CVPR)*, pages 25627–25636, 2024.
- [30] Xu Qin, Zhilin Wang, Yuanchao Bai, Xiaodong Xie, and Huizhu Jia. Ffa-net: Feature fusion attention network for single image dehazing. In *Proceedings of Association for the Advancement of Artificial Intelligence (AAAI)*, pages 11908–11915, 2020.
- [31] Yuning Cui, Wenqi Ren, Xiaochun Cao, and Alois Knoll. Focal network for image restoration. In *IEEE/CVF International Conference on Computer Vision (ICCV)*, pages 12955–12965, 2023.
- [32] Boyun Li, Yuanbiao Gou, Wenxin Wang, Peng Hu, Wangmeng Zuo, and Xi Peng. Relationship quantification of image degradations. *IEEE Trans. Pattern Anal. Mach. Intell.*, pages 1–12, 2025.
- [33] Syed Waqas Zamir, Aditya Arora, Salman H. Khan, Munawar Hayat, Fahad Shahbaz Khan, Ming-Hsuan Yang, and Ling Shao. Multi-stage progressive image restoration. In *Proceedings of IEEE/CVF Conference on Computer Vision and Pattern Recognition (CVPR)*, pages 14821–14831, 2021.
- [34] Liangyu Chen, Xiaojie Chu, Xiangyu Zhang, and Jian Sun. Simple baselines for image restoration. In *Proceedings of European Conference on Computer Vision (ECCV)*, volume 13667, pages 17–33, 2022.
- [35] Yuning Cui, Wenqi Ren, Xiaochun Cao, and Alois Knoll. Image restoration via frequency selection. *IEEE Trans. Pattern Anal. Mach. Intell.*, 46(2):1093–1108, 2024.
- [36] Yuning Cui, Wenqi Ren, Sining Yang, Xiaochun Cao, and Alois Knoll. IRNeXt: Rethinking convolutional network design for image restoration. In *Proceedings of Proceedings of International Conference on Machine Learning (ICML)*, volume 202, pages 6545–6564, 2023.
- [37] Yuning Cui, Wenqi Ren, Xiaochun Cao, and Alois Knoll. Revitalizing convolutional network for image restoration. *IEEE Trans. Pattern Anal. Mach. Intell.*, 46(12):9423–9438, 2024.
- [38] Zhi Jin, Yuwei Qiu, Kaihao Zhang, Hongdong Li, and Wenhan Luo. Mb-taylorformer v2: Improved multi-branch linear transformer expanded by taylor formula for image restoration. *IEEE Trans. Pattern Anal. Mach. Intell.*, 47(7):5990–6005, 2025.
- [39] Hanting Chen, Yunhe Wang, Tianyu Guo, Chang Xu, Yiping Deng, Zhenhua Liu, Siwei Ma, Chunjing Xu, Chao Xu, and Wen Gao. Pre-trained image processing transformer. In *Proceedings of IEEE/CVF Conference on Computer Vision and Pattern Recognition (CVPR)*, pages 12299–12310, 2021.
- [40] Jie Xiao, Xueyang Fu, Aiping Liu, Feng Wu, and Zheng-Jun Zha. Image de-raining transformer. *IEEE Trans. Pattern Anal. Mach. Intell.*, 45(11):12978–12995, 2023.
- [41] Yuda Song, Zhuqing He, Hui Qian, and Xin Du. Vision transformers for single image dehazing. *IEEE Trans. Image Process.*, 32:1927–1941, 2023.
- [42] Xiangyu Chen, Xintao Wang, Jiantao Zhou, Yu Qiao, and Chao Dong. Activating more pixels in image super-resolution transformer. In *Proceedings of IEEE/CVF Conference on Computer Vision and Pattern Recognition (CVPR)*, pages 22367–22377, 2023.
- [43] Xindong Zhang, Hui Zeng, Shi Guo, and Lei Zhang. Efficient long-range attention network for image super-resolution. In *Proceedings of European Conference on Computer Vision (ECCV)*, volume 13677, pages 649–667, 2022.
- [44] Yupeng Zhou, Zhen Li, Chun-Le Guo, Song Bai, Ming-Ming Cheng, and Qibin Hou. Srformer: Permuted self-attention for single image super-resolution. In *IEEE/CVF International Conference on Computer Vision (ICCV)*, pages 12734–12745, 2023.
- [45] Syed Waqas Zamir, Aditya Arora, Salman Khan, Munawar Hayat, Fahad Shahbaz Khan, and Ming-Hsuan Yang. Restormer: Efficient transformer for high-resolution image restoration. In *Proceedings of IEEE/CVF Conference on Computer Vision and Pattern Recognition (CVPR)*, pages 5718–5729, 2022.
- [46] Leheng Zhang, Yawei Li, Xingyu Zhou, Xiaorui Zhao, and Shuhang Gu. Transcending the limit of local window: Advanced super-resolution transformer with adaptive token dictionary. In *Proceedings of IEEE/CVF Conference on Computer Vision and Pattern Recognition (CVPR)*, pages 2856–2865, 2024.
- [47] Wei Long, Xingyu Zhou, Leheng Zhang, and Shuhang Gu. Progressive focused transformer for single image super-resolution. In *Proceedings of IEEE/CVF Conference on Computer Vision and Pattern Recognition (CVPR)*, 2025.
- [48] Yawei Li, Yuchen Fan, Xiaoyu Xiang, Denis Demandolx, Rakesh Ranjan, Radu Timofte, and Luc Van Gool. Efficient and explicit modelling of image hierarchies for image restoration. In *Proceedings of IEEE/CVF Conference on Computer Vision and Pattern Recognition (CVPR)*, pages 18278–18289, 2023.
- [49] Xiangyu Chen, Zheyuan Li, Yuandong Pu, Yihao Liu, Jiantao Zhou, Yu Qiao, and Chao Dong. A comparative study of image restoration networks for general backbone network design. In *Proceedings of European Conference on Computer Vision (ECCV)*, volume 15129, pages 74–91, 2024.
- [50] Hang Guo, Jinmin Li, Tao Dai, Zhihao Ouyang, Xudong Ren, and Shu-Tao Xia. Mambair: A simple baseline for image restoration with state-space model. In *Proceedings of European Conference on Computer Vision (ECCV)*, pages 222–241, 2024.
- [51] Hang Guo, Yong Guo, Yaohua Zha, Yulun Zhang, Wenbo Li, Tao Dai, Shu-Tao Xia, and Yawei Li. Mambairv2: Attentive state space restoration. In *Proceedings of IEEE/CVF Conference on Computer Vision and Pattern Recognition (CVPR) Workshops*, 2025.
- [52] Siyang Wang and Feng Zhao. Navigating image restoration with var’s distribution alignment prior. In *Proceedings of IEEE/CVF Conference on Computer Vision and Pattern Recognition (CVPR)*, 2025.
- [53] Qian Ning, Weisheng Dong, Xin Li, Jinjian Wu, and Guangming Shi. Uncertainty-driven loss for single image super-resolution. In

- Proceedings of Advances in Neural Information Processing Systems (NeurIPS)*, pages 16398–16409, 2021.
- [54] Ming Hong, Jianzhuang Liu, Cuihua Li, and Yanyun Qu. Uncertainty-driven dehazing network. In *Proceedings of Association for the Advancement of Artificial Intelligence (AAAI)*, pages 906–913, 2022.
- [55] Huaibo Huang, Mandi Luo, and Ran He. Memory uncertainty learning for real-world single image deraining. *IEEE Trans. Pattern Anal. Mach. Intell.*, 45(3):3446–3460, 2023.
- [56] Yuanjian Qiao, Ming-Wen Shao, Xiao-Dong Tan, and Lingzhuang Meng. Uncertainty-aware diffusion model for real-world image dehazing. In *Proceedings of Proceedings of International Conference on Machine Learning (ICML)*, pages 65–70, 2024.
- [57] Haiyan Wu, Yanyun Qu, Shaohui Lin, Jian Zhou, Ruizhi Qiao, Zhizhong Zhang, Yuan Xie, and Lizhuang Ma. Contrastive learning for compact single image dehazing. In *Proceedings of IEEE/CVF Conference on Computer Vision and Pattern Recognition (CVPR)*, pages 10551–10560, 2021.
- [58] Yu Zheng, Jiahui Zhan, Shengfeng He, Junyu Dong, and Yong Du. Curricular contrastive regularization for physics-aware single image dehazing. In *Proceedings of the IEEE/CVF Conference on Computer Vision and Pattern Recognition (CVPR)*, pages 5785–5794, 2023.
- [59] Xiang Chen, Jinshan Pan, Kui Jiang, Yufeng Li, Yufeng Huang, Caihua Kong, Longgang Dai, and Zhenhao Fan. Unpaired deep image deraining using dual contrastive learning. In *Proceedings of the IEEE/CVF Conference on Computer Vision and Pattern Recognition (CVPR)*, pages 2007–2016, 2022.
- [60] Gang Wu, Junjun Jiang, Kui Jiang, and Xianming Liu. Learning from history: Task-agnostic model contrastive learning for image restoration. In *Proceedings of Association for the Advancement of Artificial Intelligence (AAAI)*, pages 5976–5984, 2024.
- [61] Boyun Li, Xiao Liu, Peng Hu, Zhongqin Wu, Jiancheng Lv, and Xi Peng. All-in-one image restoration for unknown corruption. In *Proceedings of IEEE/CVF Conference on Computer Vision and Pattern Recognition (CVPR)*, pages 17431–17441, 2022.
- [62] Jinghao Zhang, Jie Huang, Mingde Yao, Zizheng Yang, Hu Yu, Man Zhou, and Feng Zhao. Ingredient-oriented multi-degradation learning for image restoration. In *Proceedings of IEEE/CVF Conference on Computer Vision and Pattern Recognition (CVPR)*, pages 5825–5835, 2023.
- [63] Yuning Cui, Syed Waqas Zamir, Salman H. Khan, Alois Knoll, Mubarak Shah, and Fahad Shahbaz Khan. Adair: Adaptive all-in-one image restoration via frequency mining and modulation. *CoRR*, abs/2403.14614, 2024.
- [64] Gang Wu, Junjun Jiang, Kui Jiang, Xianming Liu, and Liqiang Nie. Learning dynamic prompts for all-in-one image restoration. *IEEE Trans. Image Process.*, 34:3997–4010, 2025.
- [65] Ziwei Luo, Fredrik K. Gustafsson, Zheng Zhao, Jens Sjölund, and Thomas B. Schön. Controlling vision-language models for multi-task image restoration. In *Proceedings of Proceedings of International Conference on Learning Representations (ICLR)*, 2024.
- [66] Tian Ye, Sixiang Chen, Wenhao Chai, Zhaohu Xing, Jing Qin, Ge Lin, and Lei Zhu. Learning diffusion texture priors for image restoration. In *Proceedings of IEEE/CVF Conference on Computer Vision and Pattern Recognition (CVPR)*, pages 2524–2534, 2024.
- [67] Xu Zhang, Jiaqi Ma, Guoli Wang, Qian Zhang, Huan Zhang, and Lefei Zhang. Perceive-ir: Learning to perceive degradation better for all-in-one image restoration, 2025.
- [68] Hao Zhang, Lei Cao, Xuhui Zuo, Zhenfeng Shao, and Jiayi Ma. Omnifuse: Composite degradation-robust image fusion with language-driven semantics. *IEEE Trans. Pattern Anal. Mach. Intell.*, pages 1–18, 2025.
- [69] Alec Radford, Jong Wook Kim, Chris Hallacy, Aditya Ramesh, Gabriel Goh, Sandhini Agarwal, Girish Sastry, Amanda Askell, Pamela Mishkin, Jack Clark, Gretchen Krueger, and Ilya Sutskever. Learning transferable visual models from natural language supervision. In *Proceedings of Proceedings of International Conference on Machine Learning (ICML)*, volume 139, pages 8748–8763, 2021.
- [70] Eduard Zamfir, Zongwei Wu, Nancy Mehta, Yuedong Tan, Danda Pani Paudel, Yulun Zhang, and Radu Timofte. Complexity experts are task-discriminative learners for any image restoration. In *Proceedings of IEEE/CVF Conference on Computer Vision and Pattern Recognition (CVPR)*, 2025.
- [71] Gang Wu, Junjun Jiang, Kui Jiang, and Xianming Liu. Harmony in diversity: Improving all-in-one image restoration via multi-task collaboration. In *Proceedings of the ACM International Conference on Multimedia (ACM MM)*, pages 6015–6023, 2024.
- [72] Gang Wu, Junjun Jiang, Yijun Wang, Kui Jiang, and Xianming Liu. Debaised all-in-one image restoration with task uncertainty regularization. In *Proceedings of Association for the Advancement of Artificial Intelligence (AAAI)*, pages 8386–8394, 2025.
- [73] Xiaole Tang, Xiang Gu, Xiaoyi He, Xin Hu, and Jian Sun. Degradation-aware residual-conditioned optimal transport for unified image restoration. *IEEE Trans. Pattern Anal. Mach. Intell.*, pages 1–16, 2025.
- [74] Gang Wu, Junjun Jiang, Kui Jiang, Xianming Liu, and Liqiang Nie. Beyond degradation redundancy: Contrastive prompt learning for all-in-one image restoration. *CoRR*, abs/2504.09973, 2025.
- [75] Pablo Arbelaez, Michael Maire, Charless Fowlkes, and Jitendra Malik. Contour detection and hierarchical image segmentation. *IEEE Trans. Pattern Anal. Mach. Intell.*, 33(5):898–916, 2011-05.
- [76] Kede Ma, Zhengfang Duanmu, Qingbo Wu, Zhou Wang, Hongwei Yong, Hongliang Li, and Lei Zhang. Waterloo exploration database: New challenges for image quality assessment models. *IEEE Trans. Image Process.*, 26(2):1004–1016, 2017-02.
- [77] Boyi Li, Wenqi Ren, Dengpan Fu, Dacheng Tao, Dan Feng, Wenjun Zeng, and Zhangyang Wang. Benchmarking single-image dehazing and beyond. *IEEE Trans. Image Process.*, 28(1):492–505, 2019.
- [78] Wenhao Yang, Robby T. Tan, Jiashi Feng, Jiaying Liu, Zongming Guo, and Shuicheng Yan. Deep joint rain detection and removal from a single image. In *Proceedings of the IEEE/CVF Conference on Computer Vision and Pattern Recognition (CVPR)*, pages 1685–1694, 2017.
- [79] David R. Martin, Charless C. Fowlkes, Doron Tal, and Jitendra Malik. A database of human segmented natural images and its application to evaluating segmentation algorithms and measuring ecological statistics. In *IEEE/CVF International Conference on Computer Vision (ICCV)*, volume 2, pages 416–423, 2001.
- [80] Seungjun Nah, Tae Hyun Kim, and Kyoung Mu Lee. Deep multi-scale convolutional neural network for dynamic scene deblurring. In *Proceedings of the IEEE/CVF Conference on Computer Vision and Pattern Recognition (CVPR)*, pages 257–265, 2017.
- [81] Chen Wei, Wenjing Wang, Wenhao Yang, and Jiaying Liu. Deep retinex decomposition for low-light enhancement. In *Proceedings of The British Machine Vision Conference (BMVC)*, page 155, 2018.
- [82] Yun-Fu Liu, Da-Wei Jaw, Shih-Chia Huang, and Jenq-Neng Hwang. Desnownet: Context-aware deep network for snow removal. *IEEE Trans. Image Process.*, 27(6):3064–3073, 2018.
- [83] Rui Qian, Robby T. Tan, Wenhao Yang, Jiajun Su, and Jiaying Liu. Attentive generative adversarial network for raindrop removal from a single image. In *Proceedings of the IEEE/CVF Conference on Computer Vision and Pattern Recognition (CVPR)*, pages 2482–2491, 2018.
- [84] Ruoteng Li, Loong-Fah Cheong, and Robby T. Tan. Heavy rain image restoration: Integrating physics model and conditional adversarial learning. In *Proceedings of the IEEE/CVF Conference on Computer Vision and Pattern Recognition (CVPR)*, pages 1633–1642, 2019.
- [85] Yurui Zhu, Tianyu Wang, Xueyang Fu, Xuanyu Yang, Xin Guo, Jifeng Dai, Yu Qiao, and Xiaowei Hu. Learning weather-general and weather-specific features for image restoration under multiple adverse weather conditions. In *Proceedings of the IEEE/CVF Conference on Computer Vision and Pattern Recognition (CVPR)*, pages 21747–21758, 2023.
- [86] Xinyi Zhang, Hang Dong, Jinshan Pan, Chao Zhu, Ying Tai, Chengjie Wang, Jilin Li, Feiyue Huang, and Fei Wang. Learning to restore hazy video: A new real-world dataset and a new method. In *Proceedings of IEEE/CVF Conference on Computer Vision and Pattern Recognition (CVPR)*, pages 9239–9248, 2021.
- [87] Eirikur Agustsson and Radu Timofte. Ntire 2017 challenge on single image super-resolution: Dataset and study. In *Proceedings of IEEE/CVF Conference on Computer Vision and Pattern Recognition (CVPR) Workshops*, 2017.
- [88] Qingnan Fan, Dongdong Chen, Lu Yuan, Gang Hua, Nenghai Yu, and Baoquan Chen. A general decoupled learning framework for parameterized image operators. *IEEE Trans. Pattern Anal. Mach. Intell.*, 43(1):33–47, 2021.
- [89] Gridformer: Residual dense transformer with grid structure for image restoration in adverse weather conditions. Gridformer: Residual dense transformer with grid structure for image restoration in adverse weather conditions. *Int. J. Comput. Vis.*, pages 1–23, 2024.
- [90] Mingde Yao, Ruikang Xu, Yuanshen Guan, Jie Huang, and Zhiwei Xiong. Neural degradation representation learning for all-in-one image restoration. *IEEE Trans. Image Process.*, 33:5408–5423, 2024.
- [91] S. W. Zamir, A. Arora, S. Khan, M. Hayat, F. S. Khan, M.-H. Yang, and L. Shao. Learning enriched features for fast image restoration and enhancement. *IEEE Trans. Pattern Anal. Mach. Intell.*, 45(2):1934–1948, 2022.

- [92] Yuanhao Cai, Hao Bian, Jing Lin, Haoqian Wang, Radu Timofte, and Yulun Zhang. Retinexformer: One-stage retinex-based transformer for low-light image enhancement. In *IEEE/CVF International Conference on Computer Vision (ICCV)*, pages 12470–12479, 2023.
- [93] Lin Liu, Lingxi Xie, Xiaopeng Zhang, Shanxin Yuan, Xiangyu Chen, Wengang Zhou, Houqiang Li, and Qi Tian. TAPE: task-agnostic prior embedding for image restoration. In *Proceedings of European Conference on Computer Vision (ECCV)*, volume 13678, pages 447–464, 2022.
- [94] Jeya Maria Jose Valanarasu, Rajeev Yasarla, and Vishal M. Patel. Transweather: Transformer-based restoration of images degraded by adverse weather conditions. In *Proceedings of IEEE/CVF Conference on Computer Vision and Pattern Recognition (CVPR)*, pages 2343–2353, 2022.
- [95] Yu Guo, Yuan Gao, Yuxu Lu, Ryan Wen Liu, and Shengfeng He. Onerestore: A universal restoration framework for composite degradation. In *Proceedings of European Conference on Computer Vision (ECCV)*, pages 255–272, 2024.
- [96] Ruoteng Li, Loong-Fah Cheong, and Robby T Tan. Heavy rain image restoration: Integrating physics model and conditional adversarial learning. In *Proceedings of IEEE/CVF Conference on Computer Vision and Pattern Recognition (CVPR)*, pages 1633–1642, 2019.
- [97] Ruoteng Li, Robby T Tan, and Loong-Fah Cheong. All in one bad weather removal using architectural search. In *Proceedings of IEEE/CVF Conference on Computer Vision and Pattern Recognition (CVPR)*, pages 3175–3185, 2020.
- [98] Wei-Ting Chen, Zhi-Kai Huang, Cheng-Che Tsai, Hao-Hsiang Yang, Jian-Jiun Ding, and Sy-Yen Kuo. Learning multiple adverse weather removal via two-stage knowledge learning and multi-contrastive regularization: Toward a unified model. In *Proceedings of IEEE/CVF Conference on Computer Vision and Pattern Recognition (CVPR)*, pages 17632–17641, 2022.
- [99] Yurui Zhu, Tianyu Wang, Xueyang Fu, Xuanyu Yang, Xin Guo, Jifeng Dai, Yu Qiao, and Xiaowei Hu. Learning weather-general and weather-specific features for image restoration under multiple adverse weather conditions. In *Proceedings of IEEE/CVF Conference on Computer Vision and Pattern Recognition (CVPR)*, pages 21747–21758, 2023.
- [100] Ozan Özdenizci and Robert Legenstein. Restoring vision in adverse weather conditions with patch-based denoising diffusion models. *IEEE Trans. Pattern Anal. Mach. Intell.*, 45(8):10346–10357, 2023.
- [101] Tian Ye, Sixiang Chen, Jinbin Bai, Jun Shi, Chenghao Xue, Jingxia Jiang, Junjie Yin, Erkang Chen, and Yun Liu. Adverse weather removal with codebook priors. In *IEEE/CVF International Conference on Computer Vision (ICCV)*, pages 12619–12630, 2023.
- [102] Yuang Ai, Huaibo Huang, Xiaoqiang Zhou, Jiexiang Wang, and Ran He. Multimodal prompt perceiver: Empower adaptiveness, generalizability and fidelity for all-in-one image restoration. In *Proceedings of the IEEE/CVF Conference on Computer Vision and Pattern Recognition (CVPR)*, pages 25432–25444, 2024.
- [103] Tian Ye, Sixiang Chen, Wenhao Chai, Zhaohu Xing, Jing Qin, Ge Lin, and Lei Zhu. Learning diffusion texture priors for image restoration. In *Proceedings of IEEE/CVF Conference on Computer Vision and Pattern Recognition (CVPR)*, pages 2524–2534, 2024.
- [104] Shangquan Sun, Wenqi Ren, Xinwei Gao, Rui Wang, and Xiaochun Cao. Restoring images in adverse weather conditions via histogram transformer. In *Proceedings of European Conference on Computer Vision (ECCV)*, volume 15080, pages 111–129, 2024.
- [105] He Zhang and Vishal M Patel. Density-aware single image de-raining using a multi-stream dense network. In *Proceedings of IEEE/CVF Conference on Computer Vision and Pattern Recognition (CVPR)*, pages 695–704, 2018.
- [106] Rajeev Yasarla and Vishal M Patel. Uncertainty guided multi-scale residual learning-using a cycle spinning cnn for single image de-raining. In *Proceedings of IEEE/CVF Conference on Computer Vision and Pattern Recognition (CVPR)*, pages 8405–8414, 2019.
- [107] Wei Wei, Deyu Meng, Qian Zhao, Zongben Xu, and Ying Wu. Semi-supervised transfer learning for image rain removal. In *Proceedings of IEEE/CVF Conference on Computer Vision and Pattern Recognition (CVPR)*, pages 3877–3886, 2019.
- [108] Hongyun Gao, Xin Tao, Xiaoyong Shen, and Jiaya Jia. Dynamic scene deblurring with parameter selective sharing and nested skip connections. In *Proceedings of the IEEE/CVF Conference on Computer Vision and Pattern Recognition (CVPR)*, pages 3848–3856, 2019.
- [109] Wenqi Ren, Si Liu, Hua Zhang, Jinshan Pan, Xiaochun Cao, and Ming-Hsuan Yang. Single image dehazing via multi-scale convolutional neural networks. In *Proceedings of European Conference on Computer Vision (ECCV)*, pages 154–169, 2016.
- [110] Boyi Li, Xiulian Peng, Zhangyang Wang, Jizheng Xu, and Dan Feng. Aod-net: All-in-one dehazing network. In *IEEE/CVF International Conference on Computer Vision (ICCV)*, pages 4770–4778, 2017.
- [111] Yanyun Qu, Yizi Chen, Jingying Huang, and Yuan Xie. Enhanced pix2pix dehazing network. In *Proceedings of IEEE/CVF Conference on Computer Vision and Pattern Recognition (CVPR)*, pages 8160–8168, 2019.
- [112] Yu Dong, Yihao Liu, He Zhang, Shifeng Chen, and Yu Qiao. Fd-gan: Generative adversarial networks with fusion-discriminator for single image dehazing. In *Proceedings of Association for the Advancement of Artificial Intelligence (AAAI)*, pages 10729–10736, 2020.
- [113] Ruifan Li, Hao Chen, Fangxiang Feng, Zhanyu Ma, Xiaojie Wang, and Eduard Hovy. Dual graph convolutional networks for aspect-based sentiment analysis. In *Proceedings of Annual Meeting of the Association for Computational Linguistics (ACL)*, pages 6319–6329, 2021.
- [114] Zhiwu Huang and Luc Van Gool. A riemannian network for spd matrix learning. In *Proceedings of Association for the Advancement of Artificial Intelligence (AAAI)*, 2017.
- [115] Jinjin Gu and Chao Dong. Interpreting super-resolution networks with local attribution maps. In *Proceedings of IEEE/CVF Conference on Computer Vision and Pattern Recognition (CVPR)*, pages 9199–9208, 2021.



Gang Wu received the B.E. degree in the School of Computer Science and Technology from Soochow University, Jiangsu, China, in 2020. He is currently pursuing the Ph.D. degree in Faculty of Computing at Harbin Institute of Technology. His research interests include image restoration, representation learning, and self-supervised learning.



Junjun Jiang received the B.S. degree in Mathematics from the Huaqiao University, Quanzhou, China, in 2009, and the Ph.D. degree in Computer Science from the Wuhan University, Wuhan, China, in 2014.

From 2015 to 2018, he was an Associate Professor with the School of Computer Science, China University of Geosciences, Wuhan. From 2016 to 2018, he was a Project Researcher with the National Institute of Informatics (NII), Tokyo, Japan. He is currently a tenured professor and doctoral supervisor at the Faculty of Computing, Harbin Institute of Technology (HIT), where he also serves as Associate Dean of the School of Artificial Intelligence and Deputy Director of the Research Center for Intelligent Interfaces and Human-Computer Interaction. He is a recipient of the National Young Talents Program and leads the “Young Scientists Studio” at HIT. He has published over 100 papers in top-tier IEEE Transactions journals and CCF A conferences. His work has been cited over 20,000 times on Google Scholar, with an H-index of 66. He has been recognized as a Highly Cited Researcher globally and in China, and ranks among the top 0.05% of the world’s most influential scientists. He serves as an editorial board member of Information Fusion (recipient of the Best Editor Award in 2024), Fundamental Research, and the IEEE/CAA Journal of Automatica Sinica. His research interests include image processing and computer vision.



Kui Jiang received the M.E. and Ph.D. degrees from the School of Computer Science, Wuhan University, Wuhan, China, in 2019 and 2022, respectively. Before July 2023, he was a Research Scientist with the Cloud BU, Huawei. He is currently an Associate Professor with the School of Computer Science and Technology, Harbin Institute of Technology. He received the 2022 ACM Wuhan Doctoral Dissertation Award. His research interests include image/video processing and computer vision.



Xianming Liu received the B.S., M.S., and Ph.D. degrees in computer science from the Harbin Institute of Technology (HIT), Harbin, China, in 2006, 2008, and 2012, respectively. In 2011, he spent half a year at the Department of Electrical and Computer Engineering, McMaster University, Canada, as a Visiting Student, where he was a Post-Doctoral Fellow from 2012 to 2013. He was a Project Researcher with the National Institute of Informatics (NII), Tokyo, Japan, from 2014 to 2017. He is currently a Professor with the School of Computer Science and

Technology, HIT. His research interests include trustworthy AI, 3D signal processing and biomedical signal processing.



Liqiang Nie (Senior Member, IEEE) IAPR Fellow, is currently the dean with the School of Computer Science and Technology, Harbin Institute of Technology (Shenzhen). He received his B.Eng. and Ph.D. degree from Xi'an Jiaotong University and National University of Singapore (NUS), respectively. His research interests lie primarily in multimedia content analysis and information retrieval. Dr. Nie has co-/authored more than 100 CCF-A papers and 5 books, with 34k plus Google Scholar citations. He is an AE of IEEE TKDE, IEEE TMM, IEEE

TCSVT, ACM ToMM, and Information Science. Meanwhile, he is the regular area chair or SPC of ACM MM, NeurIPS, IJCAI and AAAI. He is a member of ICME steering committee. He has received many awards, like ACM MM and SIGIR best paper honorable mention in 2019, the AI 2000 most influential scholars2020, SIGMM rising star in 2020, MIT TR35 China 2020, DAMO Academy Young Fellow in 2020, SIGIR best student paper in 2021, first price of the provincial science and technology progress award in 2021 (rank 1), and provincial youth science and technology award in 2022. Some of his research outputs have been integrated into the products of Alibaba, Kwai, and other listed companies.